



Norwegian University of
Science and Technology

Multi-Target Stereotactic Brain Radiation Therapy

Ingrid Skarholt

Master of Science in Physics and Mathematics

Submission date: January 2018

Supervisor: Signe Danielsen, IFY

Co-supervisor: Nina Levin, St.Olav Hospital
Josefine Ståhl Kornerup, St.Olav Hospital

Norwegian University of Science and Technology
Department of Physics



Norwegian University of
Science and Technology

MULTI-TARGET STEREOTACTIC BRAIN RADIATION THERAPY
A Treatment Planning Study Comparing Linear Accelerators and Exploring New Features
in a Modern Treatment Planning System

Ingrid Kveim Skarholt

Master of Science in Biophysics and Medical Technology
Submission date: January 2018

Supervisor 1: Nina Levin, St.Olavs Hospital
Supervisor 2: Josefine Ståhl Kornerup, St.Olavs Hospital
Supervisor 3: Signe Danielsen, Department of Physics, NTNU

Abstract

Metastasis of the brain is one of the most common and severe neurological complications of cancer. Stereotactic radiation therapy (SRT) characterized by a high dose of radiation, delivered in a single or few fractions, with conformal target coverage and steep dose-falls, has been shown to be effective in treating brain metastases and recurrence gliomas. Historically, Gamma Knife (GK) has been superior to other SRT-techniques. However, the increased flexibility of the new generation of linear accelerators (linac), has made linac-SRT to a competing method. Traditionally, treatment plans for multiple-brain metastases were made with 1 isocenter pr.target. Recent studies using volumetric arc therapy (VMAT) showed about the same target coverage when optimized with single isocenter.

The aim of this study was to investigate the influence of different linear accelerator models and treatment planning strategies on irradiated volume of brain normal tissue (V_{12Gy} and V_{3Gy}), conformity (Paddick Conformity Index(PCI)) and gradient index (Dose Gradient Index(DGI)). The sensitivity of the location and number of GTVs was also studied.

Treatment plans for different linac-models and treatment planning strategies were made for 4 different multi-target brain cases. These plans were supported by the software RayStation (RaySearch Laboratories AB, v.5.99.0.5 Research). All plans were optimized with the same planning objectives, with some individual corrections for some cases, until they reached the same acceptable plan criterias

Reducing the leaf width of multi-leaf collimator (MLC) reduced the V_{12Gy} , V_{3Gy} and increased the dose gradient (DGI). However, the conformity (PCI) was reduced. Reducing the tip gap, for 5 mm leaf width, showed about the same impact on the volumes treated. It also showed higher PCI compared to the fine-leaf plans. The linac at St.Olavs, Elekta Versa HD Agility, was often the least favourable.

Single isocenter, especially when combined with new-functionalities in Raystation, showed less sensitivity to location of targets on V_{12Gy} . 1 ioscenter pr.target treated a small volume for distant GTVs, but were less favourable for close GTVs. The same sensitivity for location was seen PCI. Overall, the PCI for most treatment plans was higher than 0.75. For 1 isocenter pr.target on close GTVs PCI was lower than 0.55. The DGI was 0.2-0.3 for most plans, with some single isocenter plans as exceptions. Single isocenter treated a large V_{3Gy} , compared to the other treatment planning strategies for distant GTVs.

Based on the result of this project, decreasing the leaf width and leaf tip gap improves the flexibility of the linacs. Due to low PCI and less stability for the plans using-fine leaf, the leaf tip gap, rather than the leaf width might be of most importance. Single isocenter might be an attractive and time-effective alternative to the multiple-isocenter technique, especially when combined with new functionalities in the treatment planning system. However, when used for targets located distant to the isocenter, different methods should be tested in hope to reduce the dose spillage. This study was only based on simple cases, the trends observed must be studied further for more complex cases.

Sammendrag

Metastaser i hjernen er blant de mest vanlige og alvorlige neurologiske komplikasjonene av kreft. Stereotaktisk strålebehandling karakterisert ved høye stråledoser levert i en eller få fraksjoner, konform dose fordeling og bratt dose gradient har vist seg å være effektiv i behandling av hjernemetastaser og høygradige gliomer. Historisk sett har Gammakniven vært overlegen andre stereotaksi-teknikker. Økt fleksibilitet blant moderne lineærakseleratorer har gjort denne til en konkurrerende teknikk. Vanligvis behandles multiple- metastaser med 1 isosenter pr.svulst. Nyere forskning har vist at behandlingsplaner som benytter moderne behandlingsteknikker som volumetric arc therapy (VMAT) oppnår samme dose dekning for planer med et felles isosenter.

Målet med denne studien var å undersøke hvilken innvirkning ulike modeller av lineærakseleratorer og behandlingsstrategier hadde på bestrålt normalt hjernevev for (V_{12Gy} and V_{3Gy}), konformitet (Paddick Conformity Index(PCI)) og gradient indeks(Dose Gradient Index(DGI)). Sensitiviteten for avstanden mellom og antall svulster ble også undersøkt.

Behandlingsplaner for ulike modeller lineærakseleratorer og behandlingsstrategier ble laget for 4 ulike tilfeller av multiple-hjernemetastaser. Disse planene ble laget med programvaren RayStation (RaySearch Laboratories AB, v.5.99.0.5 Research). Alle planene ble optimalisert med de samme plan objektivene, med noen individuelle forskjeller, til de nådde kravene for å bli akseptert og ferdigstilt.

En reduksjon av bredden på Multi Leaf Collimator (MLC) reduserte V_{12Gy} , V_{3Gy} og økte dose gradienten. En reduksjon av avstanden mellom MLC-tuppene, for 5 mm tykke MLC-blader, hadde omtrent samme innvirkning på størrelsen av volumet. PCI for denne planen var også høyere enn planene der tynnere MLC-blader var brukt. Lineærakseleratoren på St.Olavs ga oftest dårlig score på de ulike evaluerings parameterne.

Felles isosenter var mindre sensitiv til avstanden mellom svulstene, spesielt når den var kombinert med nye funksjoner i Raystation, for V_{12Gy} . Multiple isosenter bestrålte et lite volum for planer med avstand mellom svulstene, men et stort volum for tette svulster. Den samme trenden ble observert for PCI. Generelt hadde de fleste planene en PCI over 0.75. Planene som brukte multiple isosenter på tette svulster hadde en PCI lavere enn 0.55. DGI lå rundt 0.2-0.3 for de fleste planene. Felles isosenter bestrålte et stort lav-dose volum, V_{3Gy} , sammenlignet med de andre behandlingsstrategier for spredte svulster.

Resultatene fra denne studien, viste at reduksjon av blad-størrelse og avstand mellom tuppene for MLC, økte fleksibiliteten til lineærakseleratoren. Lav konformitet og mindre stabilitet for planene med tynnere blader, indikerer kanskje at avstanden mellom MLC-tuppene, snarere enn bredden er det viktigste for fleksibiliteten til akseleratoren. Felles isosenter ser ut til å være et godt alternativ til multiple-isosenter teknikken, spesielt når den kombineres med nye funksjoner i planleggingssystemet. Uansett, lav dose sløsing for tilfeller med mange spredte svulster er en utfordring som må undersøkes nærmere. Denne studien undersøkte noen enkle tilfeller. Denne studien undersøkte bare enkle tilfeller. De samme planene må studeres for mer komplekse tilfeller for å se om trendene er de samme.

Preface

This report concludes my master degree in Biophysics and Medical Technology at the Norwegian University of Science and Technology, NTNU, in Trondheim. It was completed during January of 2018 and performed in collaboration with St.Olavs Hospital. The background information is partly based on the thesis "4D-CT Treatment of Lung Cancer - Photon Therapy and Proton Therapy", executed and written during the autumn of 2016.

I would like to thank my supervisors at St.Olavs Hospital Nina Levin and Josefine Ståhl Kornerup for all help and guidance during this project. I am grateful for all the assistance and advice they have given me. Without their help, positivity and enthusiasm I wouldn't have been able to complete my thesis.

I would also thank my supervisor at NTNU, Signe Danielsen, for advice and valuable feedback in the writing process. Additionally, I would like to thank Oslo Universitets-sykehus, Radiumhospitalet for giving me the opportunity to make treatment plans by using a model of one of their linear accelerators, Varian TrueBeam STx, HD-MLC 120.

Last I would like to express my gratitude to St. Olavs Hospital for providing me with the time and resources necessary to conduct my study.

Ingrid Kveim Skarholt, Trondheim,
January, 2018.

Contents

1	Introduction	1
2	Background	3
2.1	Radiation therapy equipment	3
2.1.1	Linear accelerator	3
2.1.2	Beam shaping: filters and collimators	3
2.1.3	Radiation therapy treatment techniques	5
2.2	Photon beams	5
2.2.1	Main photon interactions with matter	5
2.2.2	Photon beam description	8
2.3	Radiation therapy treatment planning process	8
2.3.1	Volumes and delineation	9
2.3.2	Treatment planning system	10
2.3.3	Dose computation	11
2.3.4	Evaluation of treatment plans	11
2.3.5	Stereotactic radiation therapy	12
3	Material and Method	15
3.1	Cases and delineation	15
3.2	Linear accelerators	16
3.3	Arc, angles and MU-settings	18
3.4	Treatment planning	18
3.4.1	1 isocenter pr.target	19
3.4.2	Single isocenter	19
3.4.3	Single isocenter and <i>treat</i>	19
3.4.4	Dose computation	20
3.4.5	Evaluation of treatment plans	20
4	Results	21
4.1	Linear accelerators	21
4.1.1	Brain dose, V_{12Gy}	21
4.1.2	Brain dose, V_{3Gy}	23
4.1.3	Paddick Conformity Index	26
4.1.4	Dose Gradient Index	26
4.2	Treatment planning strategies	26
4.2.1	Brain dose, V_{12Gy}	28
4.2.2	Brain dose, V_{3Gy}	29
4.2.3	Paddick Conformity Index	31
4.2.4	Dose Gradient Index	33

5	Discussion	35
5.1	Linear accelerators/MLC-configuration	35
5.1.1	Brain dose, V_{12Gy} and V_{3Gy}	35
5.1.2	Indexes, PCI and DGI	36
5.2	Treatment planning strategies	37
5.2.1	Brain dose, V_{12Gy} and V_{3Gy}	37
5.2.2	Indexes, PCI and DGI	38
5.3	Workflow	39
5.3.1	1 isocenter pr.target	39
5.3.2	Single isocenter	40
5.3.3	Single isocenter and <i>treat</i>	41
5.4	Limitations/Future Work	43
5.4.1	Cases and delineation	43
5.4.2	Radiation equipment	44
5.4.3	Treatment planning system	45
5.4.4	Radiobiology/risk analysis	45
5.4.5	Verification	46
6	Conclusion	47

Abbreviations

BEV Beam eye-view
CC Collapsed cone
CRT Conformal radiation therapy
CT Computed tomography
CTV Clinical target volume
DGI Dose Gradient Index
DVH(s) Dose volume histogram(s)
EBRT External beam radiation therapy
FFF Flattening filter free
GTV Gross tumor volume
HU Hounsfield units
IMRT Intensity modulated radiation therapy
ITV Internal target volume
KERMA Kinetic energy released per mass
LINAC Linear accelerator
MC Monte Carlo
MU Monitor Units
MRI Magnetic resonance imaging
MLC Multi-leaf collimator
OAR(s) Organ(s) at risk
PB Pencil beam
PCI Paddick Conformity Index
PET Positron emission tomography
PTV Planning target volume
ROI(s) Region(s) of interest
RN Radiation necrosis
RT Radiation therapy
SBRT Stereotactic body radiation therapy
SSD Source-surface-distance
SRS Stereotactic radiation surgery
SRT Stereotactic radiation therapy
TERMA Total energy released per mass
TPS Treatment planning system
VMAT Volumetric modulated arc therapy
WBRT Whole brain radiation therapy

Chapter 1

Introduction

Metastases of the brain are one of the most common neurological complications of cancer. Studies have shown an incidence of 9% –17% [53]. However, the incidence is expected to be higher, with increased probability for some types of primary cancer. Here lung, breast and melanoma cancer account for 67% –80% of the cases [53]. An exact estimate of the rate of the brain metastases is difficult to find. Studies have shown that about 170 000 of the cancer patients got intracranial metastases from a primary tumor yearly. Among them, multiple cranial metastases are presented in 70 - 80% [31]. The average survival of patients with brain-cancer is poor, typically 6 months. However, sub-groups of patients have increased probability of longer survival [52].

Intracranial Stereotactic radiation therapy (SRT) is characterized by delivery of high radiation dose in a single or a few fractions, which results in potent biological effect compared to conventional fractionation. The therapeutic ratio is optimized with a highly conformal dose distribution with steep dose fall-off, ensuring optimal absorbed dose in the target volume combined with minimal normal-tissue irradiation [18]. To achieve a dose delivery with that precision, high level and confidence in the accuracy of every steps of the treatment chain is required [46][28].

Historically, the precision required in SRT could only be obtained using Gamma Knife, introduced by the neurosurgeon Lars Leksell in 1960s. This device consisted of 179 high intensity cobalt-60 sources distributed in a hemispherical pattern and directed with extremely high precision. This model was taken over by the Elekta Corporation. The first commercial Gamma Knife model was delivered to the University of Pittsburgh in 1987 [54]. It showed a mechanical precision of 0.5 mm.

Gamma Knife (GK) has been superior to other SRT-techniques with respect to normal tissue exposure. Recently, a new generation of linear accelerators (linacs), TrueBeam STx from Varian, has been available on the market. These linacs utilize a range of treatment techniques like high definition multi-leaf collimator (HD- MLC) and high intensity flattening filter free (FFF) beams. Studies have shown that volumetric modulated arc therapy (VMAT)- plans improved the conformity, showed no significant difference in dose fall-offs, low isodose spillage or 12 Gy isodose volume. The treatment time was also significantly reduced. Linac-based SRT has been shown to be effective in treating brain metastases and recurrence gliomas [34][32][33][27].

Traditionally, VMAT-plans for multiple metastases is made with 1 isocenter pr.target. Recent studies of treatment plans optimized with a single isocenter, the geometric midpoint of all metastases, showed about the same target coverage [26].

Late toxicities leading to brain radiation necrosis (RN) is one of the most important complications related to SRT. Several factors, both related to patients and treatment, decides the probability of RN. Among the patient-related factors: tumor location, size, earlier treatments and male sex [35][36][37][38]. Some of the treatment related factors that affect the risk of RN: total dose, number of isocenters, conformality, het-

erogeneity and volume treated with given dose levels.

The aim of this study was to investigate the influence of different linear accelerator models and treatment planning strategies on irradiated volume of brain normal tissue (V_{12Gy} and V_{3Gy}), conformity and gradient index .

- How will the number and location of targets influence the treatment plans?
- Which linear accelerators and treatment planning strategies show most sensitivity to location?
- How will the treatment plans be affected by reducing the MLC-leaf width to 2.5 mm, in contrast to 5 mm? What impact has the size of the leaf tip gap?
- How robust and flexible are the different treatment planning strategies?
- Are there any drawbacks with single isocenter? Can it replace the multiple-isocenter technique?
- Can new functionalities in the treatment planning system improve the planning procedure at St.Olavs?

Chapter 2

Background

This section presents a summary of the relevant theory related to SRT, mainly focusing on the parameters evaluated in this study.

2.1 Radiation therapy equipment

2.1.1 Linear accelerator

In clinical external beam radiation therapy (EBRT), photon beams are generated from electrons passing through a linac. To gain sufficient energy, electrons from an electron gun interact with a synchronized radio frequency electromagnetic field, delivered from a magnetron. The result is high energetic electron beams, traveling close to the speed of light. A bending magnet governs the direction of the electrons. The bending system is achromatic making sure that the electrons leave the system at the same point and direction, independent of their original trajectory. A simple illustration of the linac is shown in fig. 2.1.1.

For shallow tumors, located in or near the skin, the electrons can be directed directly towards the patient. For tumors located at larger depths in the body of the patient, the electrons pass through a material with a high atomic number, often tungsten, before exiting/emerging/leaving the linac. In the tungsten block, often referred to as “target”, the electrons lose their energy in a process where photons are emitted (so called bremsstrahlung). The photons leaving the tungsten-target can be delivered from any angle by rotating the gantry and couch. The rotation of these components is centered around the isocenter: A point in space, relative to the treatment machine, where the axis of rotation of the gantry, couch and collimator intersect [1][2].

2.1.2 Beam shaping: filters and collimators

After hitting the tungsten target the photons must be focused, scattered, attenuated and shaped to be clinically useable. The main components of the linac that contributes to that process: collimation system, primary and secondary collimators, wedges, and MLC. The following section will only describe the components important for this study [6][3].

Flattening filter: The photons leaving the tungsten target are forward peaked. To achieve a more uniform beam, a flattening filter is often used, shown to the left in fig.2.1.2. The filter reduces the dose rate. It acts like a source of secondary electrons, leading to more scatter. Additionally it contributes to beam hardening, e.g changes the energy spectrum towards higher energies [1].

Historically flattened beams were commonly used, but recent years the filter is often removed to create flattening filter free (FFF) beams. FFF beams have a less uniform beam profile, shown to the right in

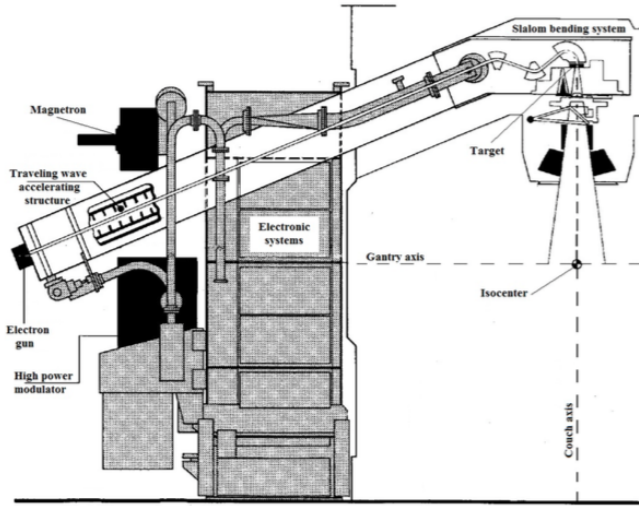


Figure 2.1.1: The main components of the linac: electron gun, magnetron, the accelerating waveguide, bending system and target [3].

fig. 2.1.2. The head scatter is reduced by approximately 70%, there are less leakage through collimators and a lower dose spillage outside the edges. Additionally, the dose rate is increased, 2-4 times faster. The reduced treatment time is especially important in time consuming treatments like SRT providing large dose per fraction. At last, without the flattening filter the beam hardening effect is not present [1].

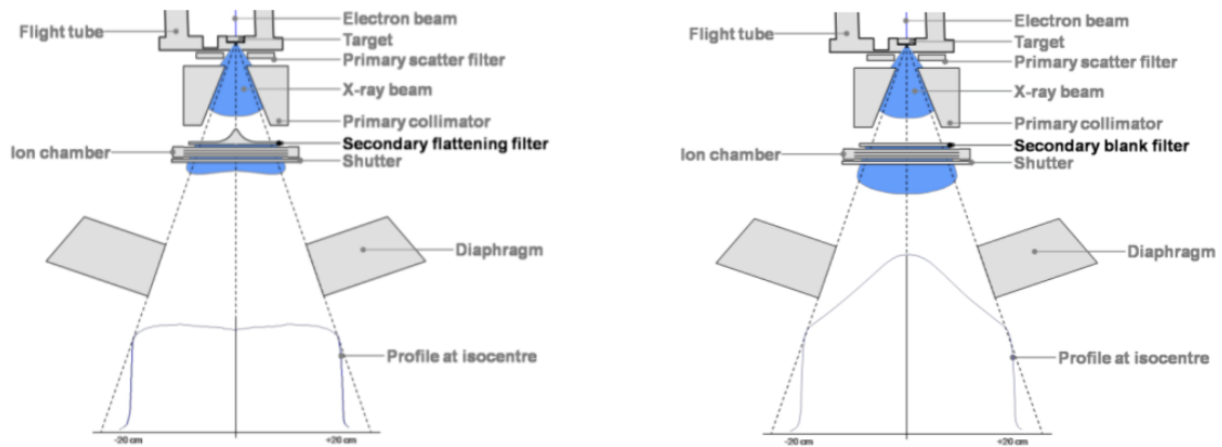


Figure 2.1.2: The resulting dose profile with and without flattening filter, respectively.

Multi-leaf collimator(MLC): The MLC consists of several pairs of metal blocks placed in opposing banks, shown in fig.2.1.3b. The beams are organized in segments, leaves, that move independent of each other. They can be moved in and out of the treatment field. Due to their rapid leaf speed of 3-6 cm/s combined with low transmission, less than 1%, they offer high flexibility in beam shaping.

MLC's from different vendors have different flexibility of movements, shown in fig.2.1.4. They differ in the their ability to overtravel e.g travel across the central axis (a), the tip gap e.g the physical distance

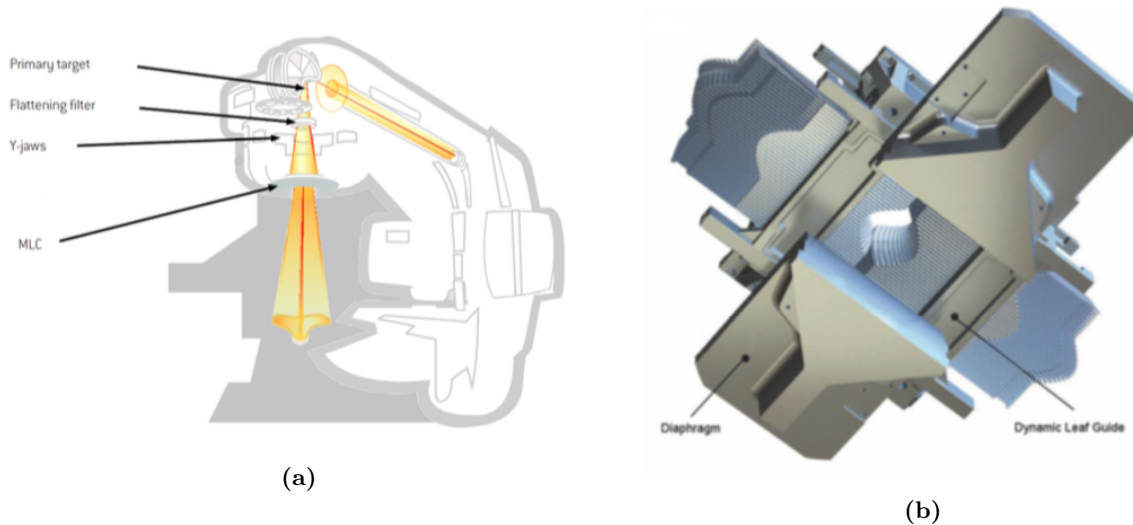


Figure 2.1.3: **a:** The travel of the photon beam through filters and collimators and at last hitting the patient [2] **b:** Illustration of the moveable leaves, dynamic wedges, called MLC [5].

between the leaf tips (b) and whether opposing leaves can move past each other, called interdigitation (c).

2.1.3 Radiation therapy treatment techniques

Many techniques have been developed to improve the conformity of EBRT. Recent years, **Intensity modulated radiation therapy (IMRT)** has been an attractive alternative. Here a discrete number of beams hits the patient from different angles. The intensity of the individual fields is modulated through a MLC, resulting in a more conform treatment.

Today the most common available technique is **Volumetric modulated arc therapy (VMAT)**, which takes the advantages of IMRT even further. VMAT is based on the same principles as IMRT, but additionally radiation is delivered continuously while the gantry rotates. The shape of MLC is continuously modulated to achieve the desired dose distribution. The gantry can rotate with an arc of 360° [16]. The speed and dose rate, Monitor Units (MU pr.time) during an arc can be controlled. The treatment time of VMAT has been shown to be about one third of IMRT [4]. The reduced treatment time is the major advantage with VMAT over IMRT.

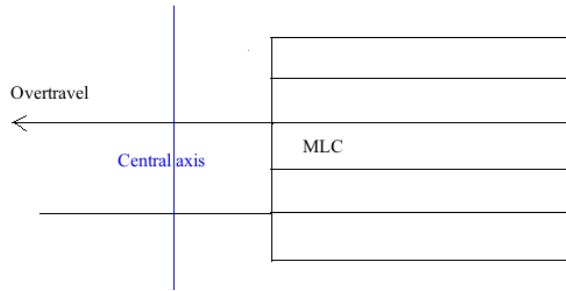
2.2 Photon beams

The following section describes the main interactions for a photon beam entering tissue for different energies.

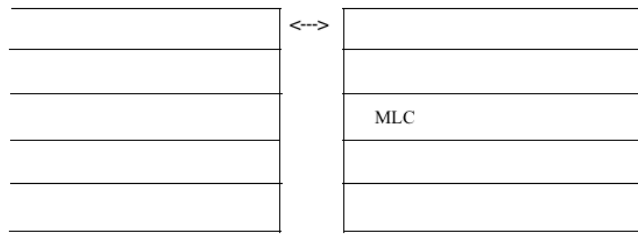
2.2.1 Main photon interactions with matter

From an ideal point source the intensity from the photon beam will decrease with $1/r^2$, where r is the source-surface distance (SSD). For a full description of the beam profile, the attenuation from travelling in a material must be taken into account. The intensity of a mono-energetic photon beam that is attenuated when passing through a material of thickness x can be described by eq. 2.1.

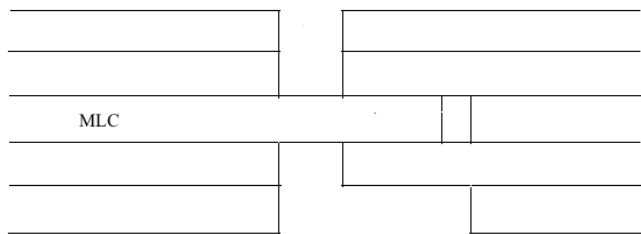
$$I(x) = I(0)e^{-\mu x} \quad (2.1)$$



(a) Overtravel
Minimum gap



(b) Gap between adjacent leaves



(c) Interdigitation

Figure 2.1.4: Characteristics of different MLC-movements

Here $I(0)$ is the intensity of an unattenuated beam, x the distance traveled and μ the linear attenuation coefficient.

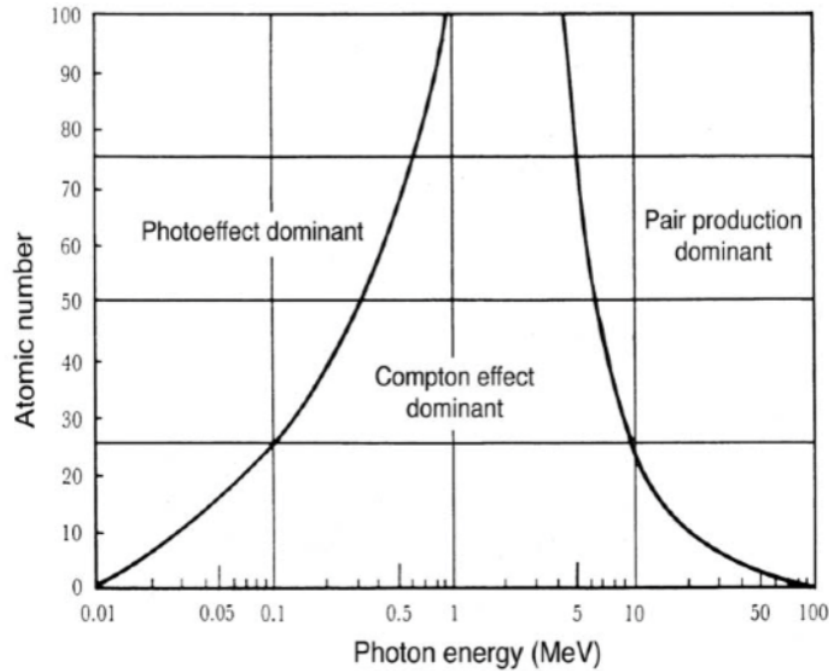


Figure 2.2.1: The three main interaction processes with between photons and matter and their dependence on energy and atomic Z-number of the material. The drawn lines represent areas where two processes are equally probable [12].

Photons interact with matter in three main ways: photoelectric effect, Compton scattering and pair production. As shown in fig.2.2.1 the probability of which interaction taking place is highly dependent on the atomic Z-number of the material and energy of the photon, E_γ . The clinical photon beams used in this project will have a maximum energy of 6 MeV, with an average energy about 1/3 of the max. In this energy range the Compton effect dominates. Here a photon with incident energy E_γ transfer some of its energy to the atom, releasing a recoil electron. The remaining energy E_γ' and released electron continue in further reactions [8][9].

The kinetic energy transferred from photons to the secondary charged particles, quantified as kinetic energy released per mass (KERMA), does not contribute directly to dose. Instead, the energy deposition due to interactions of the released electrons with matter defines the dose. Photons and electrons transfer their energy to matter via atomic excitations or ionizations. The energy deposition can be described by the stopping power of the material. According to eq. 2.2, it is defined as the average loss of energy E , per unit path length, x . The negative sign makes the stopping power positive.

$$S(x) = -\frac{dE}{dx} \quad (2.2)$$

Stopping power can be divided into two sub-groups: radiative and collision. Reactions with atomic nuclei are radiative stopping power, while reactions with orbital electrons are collision stopping power. Divided by the mass density of the medium results in mass stopping power [MeVcm²/g], that describes the dose [1][7].

2.2.2 Photon beam description

Photons are attenuated exponentially in matter, eq.2.1, with dose decrease exponentially with depth of penetration. Additionally the linear attenuation coefficient decreases with increasing energy, then the beam of higher E will be more penetrating e.g go deeper into the tissue for the same dose level [10][11][12].

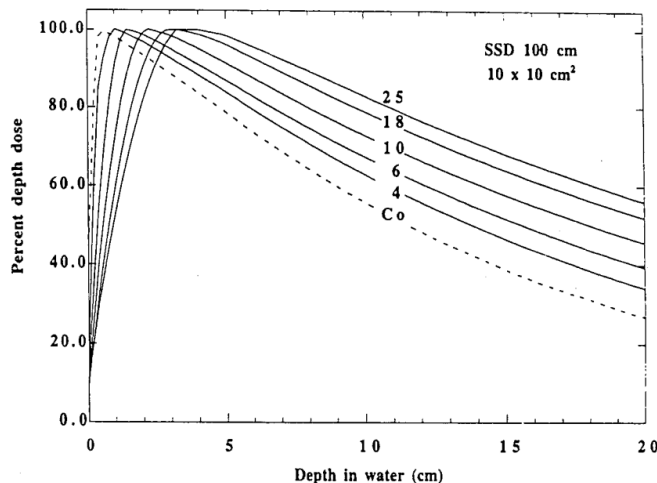


Figure 2.2.2: The depth dose of photon beams with different energies. Photon beam of higher energy are more penetrating, leading to a shift of the curve to the right.

Since Compton scattering only is a starting point for interaction with matter, followed by a number of ionizations caused by the charged particles released, the energy is not absorbed at the location of the first photon interaction. This results in a phenomena called a buildup region, shown in fig.2.2.2 that illustrate depth dose curves for different photon energies. Photons with increased energy will be more penetrating, e.g go deeper into tissue before interacting. Then, the buildup region is moved to the right. The build up effect is also essential for photons traveling between different medium. The lack of electronic equilibrium between the interfaces will cause a buildup region [10][11][12][13].

2.3 Radiation therapy treatment planning process

The following section describes the main steps in the radiotherapy treatment planning process.

The first step is to acquire a three-dimensional (3D) computed tomography (CT) image to get information about the electron density. Then delineate volumes/regions of interest (ROIs), often with aid from magnetic resonance imaging (MRI), positron-emission tomography (PET) or other imaging modalities. Then create a treatment plan (inversely optimized or forward planning) based on prescribed dose and normal tissue tolerances.

CT images provide information about the patient mass density from Hounsfield units (HU). The HU-scale is a linear transformation of the linear attenuation coefficient μ , in x-, y- and z-direction, at the energies of the CT-scanner.

$$HU = 1000 \cdot \frac{\mu - \mu_{H_2O}}{\mu_{H_2O}} \quad (2.3)$$

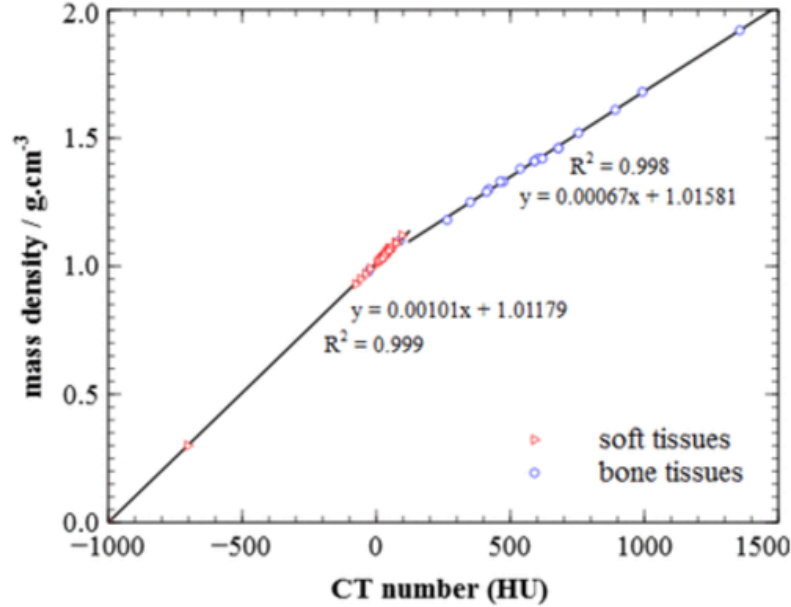


Figure 2.3.1: The correlation between HU-scale and density.

HU in distilled water at standard pressure and temperature is defined as zero. Air is -1000. CT-scanners are therefore calibrated based on the HU-reference of water.

Anatomical structures have standard HU-values, blood (+30 to +45), muscle (+40), lungs (-950 to -550) and liver (+50 to +70). The HU-values for different materials have a direct correlation with density. The mass density in each voxel is converted from the HU-scale, as seen in fig. 2.3.1 [23][24].

2.3.1 Volumes and delineation

The volumes, margins and parameters used in clinical practice are based on guidelines from KVIST¹ group and NRPA², closely related international recommendation from ICRU³ [14][15].

Target volumes are based on recommendations in the ICRU Report 83 [14][15]. All volumes, shown in fig. 2.3.2, are related to the tumor with an additional margin, that includes different factors and uncertainties influencing the size of tumor volume.

Gross tumor volume (GTV) is the primary tumor or metastasis, places with high density of malignant cells.

Clinical target volume (CTV) includes GTV and a margin with high probability of malignant growth and subclinical disease. The volume delineation uses data from protocols as hint markers.

Internal target volume (ITV) is generated by adding a margin that includes inter- and intra-fractional changes in CTV. During the treatment period, lasting for several weeks, factors like weight loss and tumor

¹KVIST- Quality Assurance in Radiation Therapy (In norwegian: Kvalitetssikring i stråleterapi)

²NACP- Nordic Association of Clinical Physics

³ICRU- International Commission on Radiation Units and Measurements

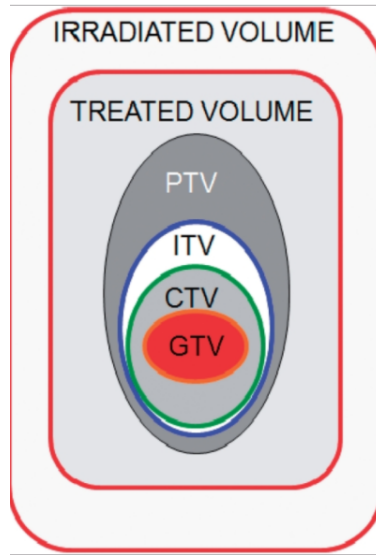


Figure 2.3.2: The target volumes in radiation therapy recommended in the ICRU Report 83 [14][15].

shrinkage may affect shape, size and position of CTV. Additionally, for tumors in the lung region especially, periodic motion like heart beat and breathing must be taken into account. Random motion like peristalsis and bladder filling may also influence the delineation process.

Planning target volume (PTV) is the ITV enclosed by a margin accounting for systematic and random errors in patient-setup and treatment machine. This can be uncertainties in patient positioning, image transfer, dose calculation algorithms and calibration of the treatment machine. Systematic errors depend on local conditions, and will influence all treatments. In some cases however, PTV is directly outlined from CTV, and the ITV is not defined.

Organs at risk ((OARs): In RT the dose to all normal tissue should be limited. Some structures, however are so sensitive to radiation that they must be critically examined in treatment planning. For serial structures, like the spinal cord, dose only to a small region, a few subunits, can lead to loss in function. Parallel structures, like the lung and liver, a large region of the volume must be irradiated before functional loss. On the other hand, with the whole volume irradiated, these structures are very sensitive to radiation [1][14][15]. For SRS of the spinal cord Brainstem, optical nerves, eye lenses and chiasm are examples of structures that must be critically examined[?]

2.3.2 Treatment planning system

After the doctor has delineated the target volumes, the OARs and determined the prescription dose, the correct treatment modality and the energy of the clinical beams must be chosen. Then the number of arcs with their respective angles are set. Later the radiation output, both the time and Monitor Units (MU) can be controlled [6].

Then the treatment planner (usually a radiation therapist or physicist), selects a set of objectives and/or constraints to guide/steer the optimization process, and control the target coverage and the doses OARs [6]. The treatment planning system (TPS) tries to find an optimal solution improving the objectives as much as possible until the user-defined maximum number of iterations are reached or when the optimal solution is found [6].

2.3.3 Dose computation

Monte Carlo (MC) is the most accurate method to compute doses in radiotherapy. Monte Carlo follows a particle through its interactions until all energy is lost, e.g. deposited. The algorithm simulates a stochastic process by averaging over a large number of stories with known probability distribution. Here interaction, energy, direction and distance to next interaction are included. The main drawback with MC is that it requires huge computer power and might be very time consuming [17].

Since the MC-algorithm is very time consuming, methods using energy kernels, describing the dose distribution in a point (point kernels) or along a ray line (pencil beam), are preferred. As an example, Collapsed Cone (CC) uses a weighted sum of monoenergetic point kernels. It calculates the effective radiological depth, scaled for inhomogeneities, both laterally and in the primary fluence direction. A simple illustration is shown in fig.2.3.3. The absorbed dose is computed by the convolution of total energy released per mass (TERMA) and the dose deposition kernel. According to recommendations in KVIST, excluding lateral scatter does not give a precise description of dose. For the treatment plans made in this study, CC was the preferred method [17].

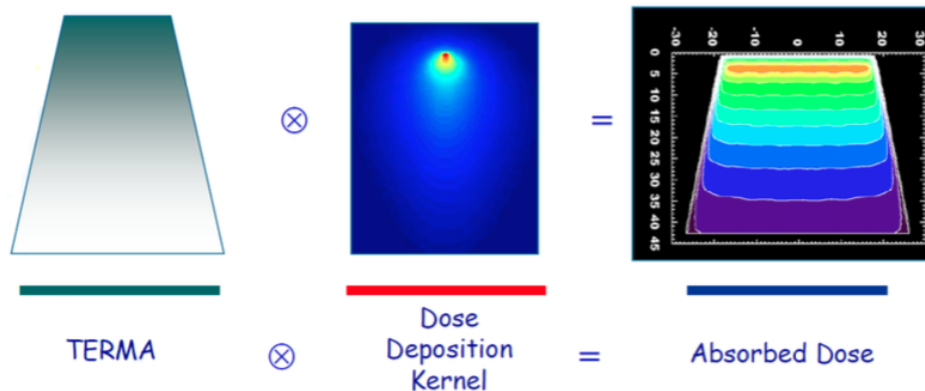


Figure 2.3.3: The absorbed dose is calculated from the convolution of TERMA and the dose deposition kernel. The illustration is taken from a presentation in the course FY8409 at NTNU.

2.3.4 Evaluation of treatment plans

A dose volume histogram (DVH), shown in fig.2.3.4, illustrates parameters describing different relations between irradiated volume and dose. D_V represents the minimum dose D , to a volume V , while V_D is the volume V receiving a dose D or higher. These values can be illustrated absolute or relative to a reference value. $D_{2\%}$ is the clinical representation of D_{max} . $D_{98\%}$, on the other hand, defines D_{min} . These parameters indicate the highest and lowest dose, respectively, within a volume of interest. Sometimes, $D_{2\%}$ might be too small or it is important to know the exact volume. Then, if necessary the volume can be reported as dose to absolute volume, 35 mm^3 for SRT [18]. For the OAR listed in section 2.3.1, $D_{2\%}$ is relevant for serial structures. Here $D_{2\%}$ might be too large, and should be reported in a smaller volume. Parallel structures are best described with D_{mean} . Another parameter to register is D_{mean} which represents the average of all voxels inside a defined volume [14] [18].

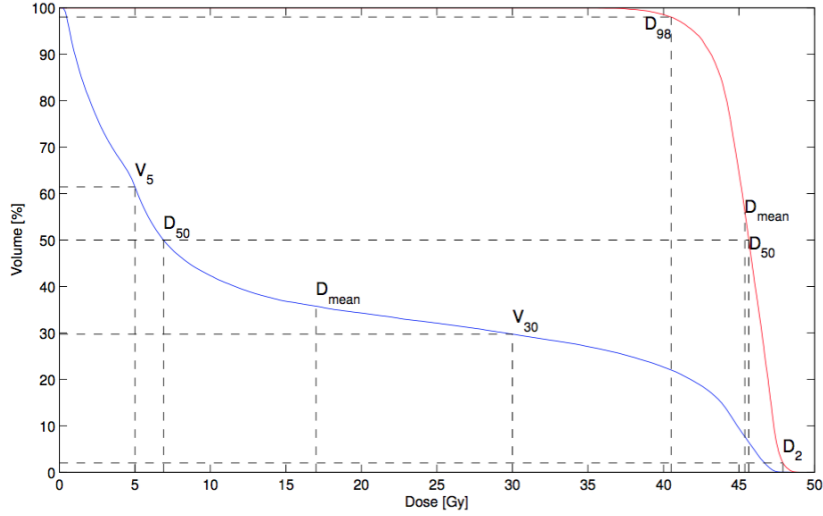


Figure 2.3.4: Example of a dose volume histogram with some dose - and volume parameters. The red curve illustrates the parameters described in section, $D_{2\%}$, $D_{98\%}$ and D_{mean} .

The quality of a treatment plan can be evaluated by many indexes. For SRT indexes describing conformity and gradient are of most importance.

Dose conformity is defined as the degree of which the high dose region conforms the target volume. The Conformity Index has been calculated in different ways, often reported as the ratio of the prescription isodose volume to target volume. A common drawback for all the different definitions, they do not take possible under-treatment into consideration. To overcome that limit, Paddick et.al [19] developed a new index described by equation 2.4. The ideal value of **Paddick Conformity Index (PCI)** is 1.

$$PCI = \frac{TV_{PIV}^2}{TV * PIV} \quad (2.4)$$

Here TV_{PIV} is the part of the target volume receiving the prescription isodose. Then, TV is the target volume and PIV the total volume receiving the prescription isodose.

A measure of the dose gradient outside PTVs is described by **Dose Gradient Index (DGI)**, is described by eq. 2.5 [18].

$$DGI = \frac{V_{100\%}}{V_{50\%}} \quad (2.5)$$

Here $V_{100\%}$ represent the volume covered with 100% with the prescription isodose, while $V_{50\%}$ is the volume covered with 50% of the same isodose.

DGI should ideally be 1. However, a dose fall-off with that sharp gradient is impossible.

2.3.5 Stereotactic radiation therapy

Intracranial SRT is characterized by delivery of a high radiation dose in a single or a few fractions to a well-defined volume. The therapeutic ratio is optimized with a highly conformal dose distribution with steep

dose fall-off, ensuring optimal absorbed dose in the target volume combined with minimal normal-tissue irradiation [18][46][28]. SRT is mostly used to treat small planning targets. The prescribed dose is 10-50 Gy, delivered in one or several fractions [1].

In conventional therapy the main rationale for fractionation is to spare the dose to normal tissue. Each fraction repeat the shoulder of the survival curve. Classical radiobiology is described by the 5 Rs: repair, repopulation, redistribution, reassortment and reoxygenation.

The radiobiological principles making fractionation cannot describe the effectiveness of SRT. In addition to the direct kill of tumor cells, destroying the strands of DNA, indirect killing is also possible. Studies have shown that the tumor cells killed, indirectly and directly, in SRT release tumor antigens. These antigens stimulate anti-tumor immunity that again suppress the recurrence and metastatic growth [20]. Other studies has shown that irradiation destroys vasculators. A deteriorating intra-tumor microenvironment leads to secondary tumor cell death [21] [22] .

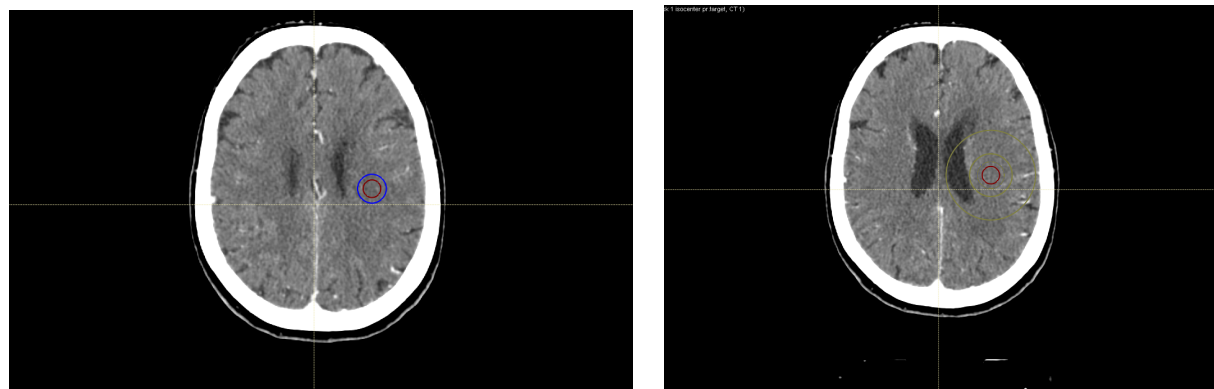
Late toxicities leading to RN is is one of the most important complications related to SRT. The risk of RN depends on a variety of factors: radiosurgical techniques, type of lesion, patient selection etc. some good risk predictors have been found. The Quantec-report [25] stated that V_{12Gy} should be the standard method of reporting dose to normal brain in radiosurgery procedures. To minimize the risk of RN this volume should not be higher than 10 cm^3 .

Chapter 3

Material and Method

Treatment plans were made for 4 different multi-target brain-cases for different linac-models and treatment planning strategies. All plans, independent of linac, treatment planning strategy and location of GTVs, had the same optimization objectives and criterias to evaluate an acceptable plan.

3.1 Cases and delineation



(a) GTV (red) with a margin of 3 mm to make PTV (blue).

(b) The ring structures (green).

Figure 3.1.1: Volumes and structures for case 1, in transversal direction.

4 different multi-target brain cases were generated from the same set of CT-images, with a slice thickness of 1 mm. The number (2 or 3) and location (close or distant) of metastases varied, while all were spheres with a radius of 6 mm, yielding a volume of 2.90 cm^3 . All metastases were delineated as GTVs. According to the procedure for Stereotactic treatment planning at St. Olavs Hospital, margins and structures should be drawn to control the dose distribution. First, a margin of 3 mm was drawn around each GTV to make PTV. Additionally two different ring structures were created. These rings were used to control the dose fall-off for the volume outside PTV. The first ring, Ring 1, ranged 0.5 cm outside PTV. The second ring, Ring 2, started at Ring 1 and ranged 1.5 cm, 2 cm outside PTV. All structures are shown in fig. 3.1.1(CT-image) and 3.1.2(simple illustration). None of the GTVs were located close to critical structures. Normal brain tissue, defined as $\text{Brain} - \text{PTV}_{\text{union}}$, with $\text{PTV}_{\text{union}}$ as the union of all PTV-volumes of the respective case, was the OAR for this project. This volume differs, dependent on the number of PTVs, but will be called **OAR Brain** in the project.

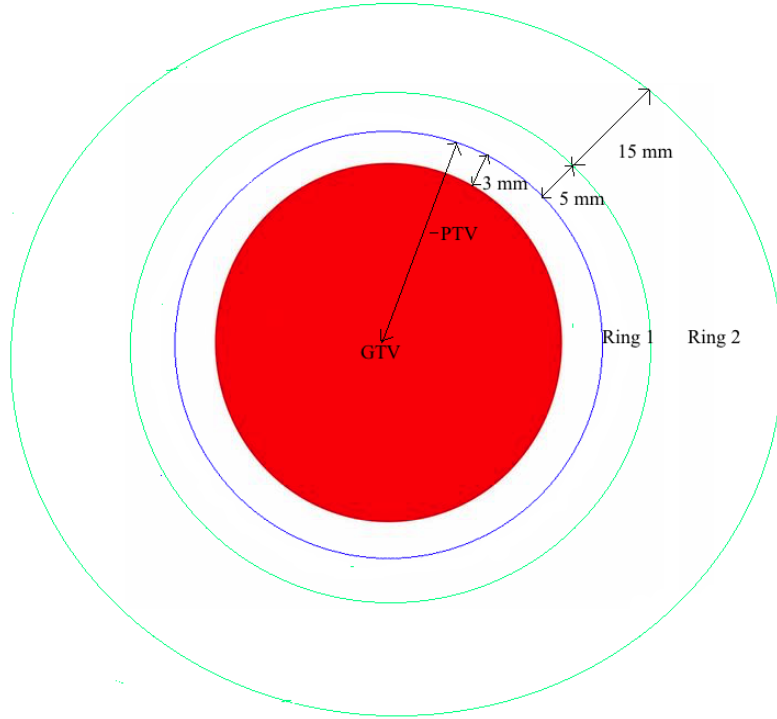


Figure 3.1.2: Illustration of GTV, PTV and the ring structures with their respective sizes.

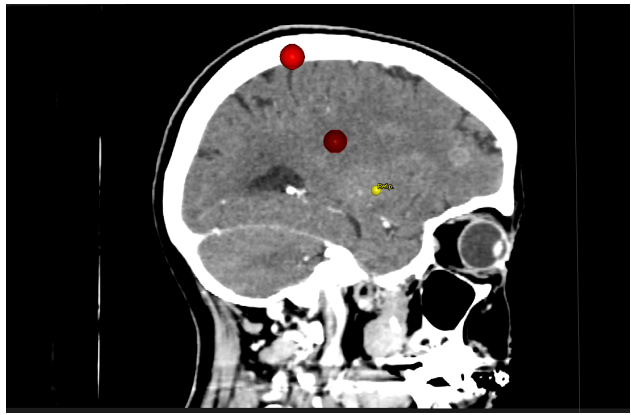
The cases were divided into two groups depending on the number of targets. 2 metastases for case 1 and 2, while 3 metastases for case 3 and 4. Additionally they could be separated based on location. For case 1 and 3 the metastases were located far away from each other, while case 2 and 4 the metastases were located close to each other. An illustration of all cases with number and location of GTVs is shown in fig. 3.1.3.

For cases with distant GTVs (1 and 3) none of the structures were overlapping. For cases with close GTVs (2 and 4) on the other hand, the rings from different metastases were overlapping. As shown to the left in fig. 3.1.4, the ring structure that belonged to PTV_1 was overlapping with PTV_2 . Situations like that, where volumes that should have high dose with respect to one PTV, but low dose with respect to the other, were complicated. To avoid competing optimization objectives, a union of the rings enclosing the union of PTVs were made, shown to the right in fig. 3.1.4.

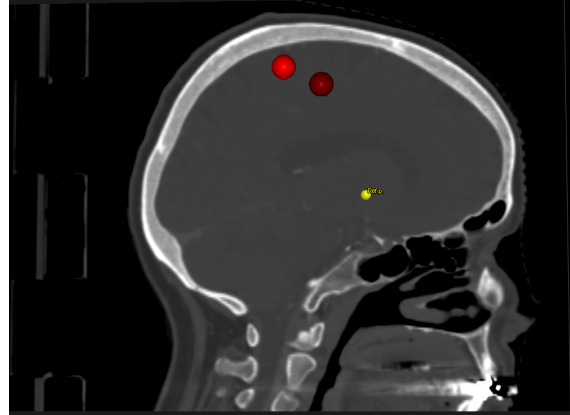
3.2 Linear accelerators

Table 3.2.1: The most interesting differences (for this project) between the linacs: leaf width and gap.

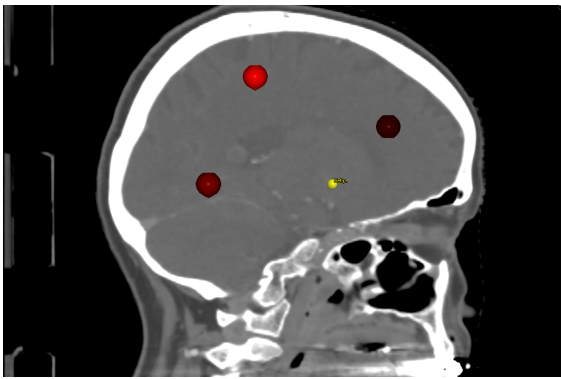
Linear accelerator	Leaf width [mm]	Leaf gap [mm]	[#]
Elekta (10 mm gap)	5	10	1
Elekta (5 mm gap)	5	5	2
Varian (2.5 mm)	2.5	1	3



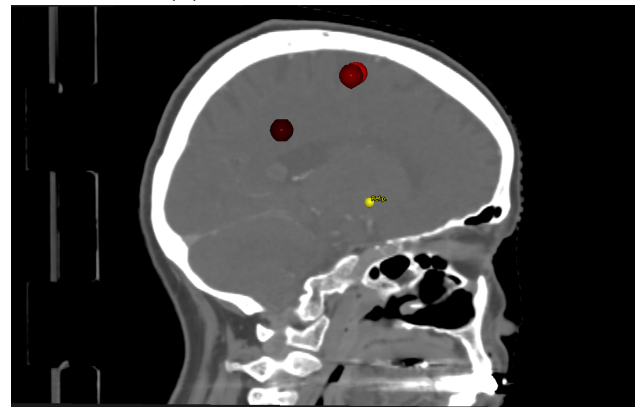
(a) Case 1, sagittal direction



(b) Case 2, sagittal direction

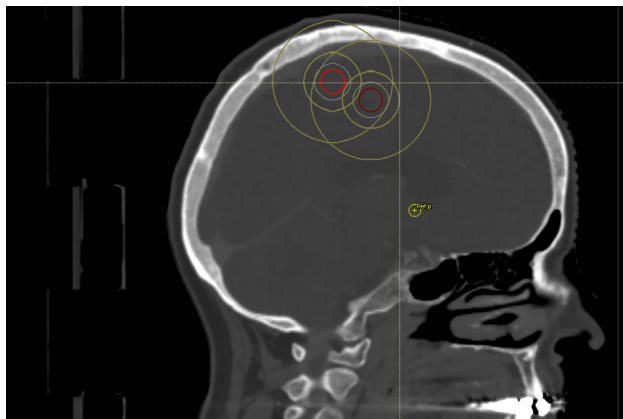


(c) Case 3, sagittal direction

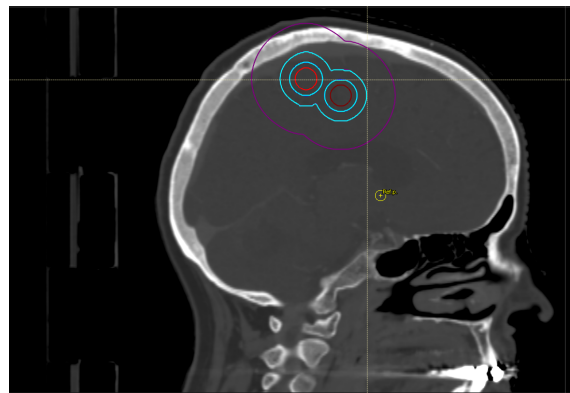


(d) Case 4, sagittal direction

Figure 3.1.3: Top row: Cases with 2 targets located distant (a) and close (b) to each other. Bottom row: 3 targets located distant (c) and close (d) to each other.



(a) Original structure: Overlap of the rings



(b) New structure: Union of the rings

Figure 3.1.4: Illustration of the ring structures for case 2.

The plans were optimized for 3 linac-models that varied in leaf gap and width of the MLC-leaves. First, all plans were optimized in the treatment planning system by the linac available at St.Olavs, Elekta Versa HD Agility. This linac had MLC-leaf width of 5 mm and a leaf tip gap of 10 mm. Later, the same plans were made for a modified version, that differed in the leaf tip gap, of the same linac. This linac had a distance of 1 mm between the tips, projected to 5 mm at the isocenter, 100 cm. For this project, the linac at St. Olavs is called **Elekta (10 mm gap)** and the modified linac, **Elekta (5 mm gap)**. At last, the plans were optimized for a linac-model from OUS (Oslo Universitets Sykehus, Radiumhospitalet), Varian TrueBeam STx, HD-MLC 120. Compared to the linacs from Elekta, it varied in both leaf width, 2.5 mm, and tip gap, 1 mm. This linac is called **Varian (2.5 mm)** in the project. An overview over the different linacs, their leaf width and gap of MLC is shown in tab. 3.2.1.

3.3 Arc, angles and MU-settings

Table 3.3.1: The arcs pr.target with their respectively gantry- , couch angles and directions.

Arc/Beam	Couch angle	Gantry angle	Direction
1	0	178-182	CCW
2	30	182-0	CW
3	330	0-178	CW

The radiation from the 2 linacs was 6 MV FFF beams. As described in section 2.1.2, using FFF- beams increases the dose rate which is favorable in treatments with large fractions of dose, as SRT. According to the procedure from St.Olavs Hospital, VMAT was chosen as radiation treatment technique. Here a beam set of 3 arcs pr. target was used. The settings of the arcs are shown in tab. 3.3.1. The direction was either clockwise (CW) or counterclockwise (CCW).

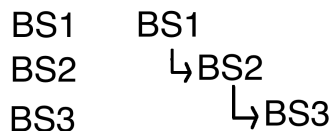
The collimator angle was 5 degrees for all arcs. The monitor units (MU) was controlled to give about half of MU to arc 1, and about 1/4 to each of the two other arcs, 2 and 3. To make sure that the MLC-movement between two control points does not change dramatically, the leaf motion of MLC was limited. For both Elekta and Varian’s system this was set to 2 cm/4 degrees, e.g 0.5 cm/deg [3].

3.4 Treatment planning

Table 3.4.1: The treatment planning strategies used in this project.

Treatment planning strategy	[*]
1 isocenter pr.target	a
Single isocenter	b
Single isocenter and <i>treat</i>	c

Treatment plans with 3 different treatment strategies were made. All plans were optimized in the software program RayStation (RaySearch Laboratories AB, v.5.99.0.5 Research). The treatment strategies were **1 isocenter pr.target**, **single isocenter** and **single isocenter with *treat***, shown in tab. 3.4.1. *Treat* is a new function in Raystation, where the user can choose which targets the different arcs should treat in the optimization. For Elekta (10 mm gap) the *treat*-function lead to programming errors and unwanted exits in Raystation. Elekta (10 mm gap) was therefore planned with 1 isocenter pr.target and single isocenter only.



$$\text{Plan dose} = \text{BS1} + \text{BS2} + \text{BS3}$$

Figure 3.4.1: The dependency of the different beamsets used for 1 isocenter pr.target

3.4.1 1 isocenter pr.target

As shown in fig.3.4.1, were made with 3 independent beams sets (BS1, BS2, BS3) that treated a PTV₁, PTV₂ and PTV₂ respectively. Each beamset consisted of the arcs listed in table 3.3.1. The isocenter of these arcs were set to the geometric center of the target treated by the respective beamset.

To optimize the treatment plan a number of objectives were added in the TPS. All objectives are listed in table 3.4.2. As shown to the left in fig. 3.4.1, the dose to the first target these was related to the individual beamset. For the second target, the background dose from BS1 was included. For the third target, the background dose from both beamset, BS1 and BS2, were included. However, the dose contribution from other beamsets were reduced by adding an max-objective.

The optimization was stopped when the criterias for an acceptable plan was fulfilled. 100% of GTV should be covered with 21.4 Gy, while 18 Gy should cover at least 98% of the PTV. The max dose, D_{2%}, should not be higher than 27 Gy. The criterias for accepting a plan had to be fulfilled for the plan dose, defined as the sum of the doses from the different beamsets. not necessarily for the individual beam set.

Table 3.4.2: The optimization objectives...

Target/Volume	Objective	Dose level [Gy]	Distance [cm]
GTV	Minimum dose	21.4	
PTV	Minimum dose	18	
PTV	Maximum dose	27	
Ring 1	Dose fall off	18-9	0-0.5
Ring 2	Dose fall off	9-3	0.5-2

3.4.2 Single isocenter

For the treatment plans with single isocenter the 3 arcs listed in table3.3.1 were multiplied with the number of targets, e.g on average 3 arcs pr.target. The isocenter of all arcs were set to the geometric center of the the union of GTVs. The objectives listed in tab. 3.4.2, was related to each of the targets, and all criteria were based on the plan dose. Then some targets were more favourable than others. For a plan to be accepted, each at least 98% of each PTV was covered with 18 Gy. The total volume of GTV, 100%, was covered with covered with 21. 4 Gy.

3.4.3 Single isocenter and *treat*

Treat-functionality in Raystation controlled the behaviour of the MLC-leaves. This was done by setting margins in the moving direction(y) of MLC, shown in fig.3.4.2. The main goal was to limit the distance between MLC-leaves and PTV e.g let the MLC-leaves move close to the target. A margin of 0.4 cm was

chosen to avoid programming-errors. Which and how many targets that was controlled by the different beams was decided by the user. In this project each beam controlled one target only. The order of beams was effectively 3 beams (tab. 3.3.1) pr.target. The treatment plans had the same objectives as the plans with other treatment planning strategies, listed in tab. 3.4.2. As for single isocenter the PTV-coverage was at least 98% and GTV 100% if possible.

Name	Margins [cm]				Treat	
	X1	X2	Y1	Y2	PTV1	PTV2
1	0.00	0.00	0.40	0.40	<input checked="" type="checkbox"/>	<input type="checkbox"/>
2	0.00	0.00	0.40	0.40	<input checked="" type="checkbox"/>	<input type="checkbox"/>
3	0.00	0.00	0.40	0.40	<input checked="" type="checkbox"/>	<input type="checkbox"/>
4	0.00	0.00	0.40	0.40	<input type="checkbox"/>	<input checked="" type="checkbox"/>
5	0.00	0.00	0.40	0.40	<input type="checkbox"/>	<input checked="" type="checkbox"/>
6	0.00	0.00	0.40	0.40	<input type="checkbox"/>	<input checked="" type="checkbox"/>

Figure 3.4.2: Illustration of the variables/margins that is controlled with the treat function

3.4.4 Dose computation

The dose for all cases, linacs and treatment planning strategies were computed with the CC-algorithm. The dose matrix/resolution was set to 0.2 cm in all three directions(right-left, inferior-superior, posterior-anterior). The optimization tolerance was set to 1.000E-7.

3.4.5 Evaluation of treatment plans

An overview of the different cases, linacs, treatment planning strategies is shown in table 3.4.3. Details of linac-model (represented by number) can be seen in 3.2.1 and treatment planning strategies (represented by letters) can be seen in 3.4.1.

All plans were evaluated with a number of parameters related to brain dose, V_{12Gy} , V_{3Gy} , target con-

Case [#]	Number and location of targets	Treatment plans [#][*]
1	2- distant	1.a,b), 2.a,b,c), 3.a,b,c)
2	2- close	1.a,b), 2.a,b,c), 3.a,b,c)
3	3- distant	1.a,b), 2.a,b,c), 3.a,b,c)
4	3 - close	1.a,b), 2.a,b,c), 3.a,b,c)

Table 3.4.3: An overview of the treatment plans optimized and evaluated in the project. Information about the cases, linacs, treatment planning strategies, parameters and indexes are listed in the table. # indicate the id of the linac (tab.3.2.1), while * is the treatment planning strategy (tab.3.4.1)

formity, PCI, and dose fall off, DGI. The volume evaluated for V_{12Gy} , V_{3Gy} was OAR Brain. The indexes were calculated according to the formulas given in section 2.3.4. Ideally, for multiple-metastases a PCI and DGI should be calculated for each target. However, in these cases dose regions from the different targets blend into each other. Then global indexes based on the union of target volumes were calculated

Chapter 4

Results

This section presents the most interesting results and trends when comparing the different linac-models and treatment planning strategies. The influence of number and location of targets is also studied. All treatment plans with their respective treatment planning strategy, linac-model, number and location of targets are listed in tab. 3.4.3.

The quality of a treatment plan was evaluated by the values of the parameters and indexes described in section 3.4.5. Then "good quality" refers to small volume treated, with 12 or 3 Gy, high degree of target coverage (high PCI) and sharp dose fall-offs (high DGI).

4.1 Linear accelerators

The following section compares treatment plans optimized by the same treatment planning strategy, but different linac- models: **Elekta (10 mm gap)**, **Elekta (5 mm gap)** and **Varian (2.5 mm)**. Detailed information about the different linac-models is shown in table 3.2.1. Important to note, as mentioned in section 3.4, the *treat*-functionality did not work for Elekta (10 mm gap). For plans using single isocenter and *treat*, Elekta (5 mm gap) and Varian (2.5 mm) were the only linac-models compared.

4.1.1 Brain dose, V_{12Gy}

The impact of different linac-models for normal brain tissue (OAR Brain) treated with 12 Gy or more (V_{12Gy}) can be seen in fig. 4.1.1. As described in section 4.1.1, V_{12Gy} should not override 10 cm^3 . To study which treatment plans that fulfill this criteria the limit is represented by a black line.

For treatment plans with **1 isocenter pr.target** fig. 4.1.1 (a), the V_{12Gy} was sensitive to location of GTVs for all linac-models. The plans using Elekta (10 mm gap) (blue) showed most difference between the plans for close- (star) and distant-GTVs (circle). The plans using Elekta (5 mm gap) (green) were less influenced by the distance between GTVs.

Overall, plans for distant GTVs (circles) gave a lower dose compared to the plans for close GTVs (stars) based on cases with the same number of targets. Varian (2.5 mm) (red circle) treated the smallest volume for all plans with distant-GTVs, while Elekta (5 mm gap) (green circle) treated the largest volume. The treatment plans for 2 distant targets, almost fulfilled the V_{12Gy} -criteria for all linac-models.

For the plans with close GTVs, Elekta (10 mm gap) treated the largest volume, most clearly seen for 3 close targets (blue star). This plan showed great difference from the other plans optimized for the same case. Consequently, it treated more than 55% more normal brain tissue compared to the two other linac-models. This plan had a sub-optimal plan quality, e.g did not fulfill acceptable plan criteria, that will be discussed

later.

The influence of different linac-models when using a **single isocenter** as planning strategy is shown in fig. 4.1.1 (b). Compared to (a), a clear difference in volume treated between plans with distant and close GTVs was not observed. Overall, the quality of the treatment plans with single isocenter was less influenced by location.

The cases with 2 targets showed about the same trend with respect to choice of linac. The plans with Elekta (10 mm gap) (blue stars and circles) treated the largest volume, while Elekta (5 mm gap) (green stars and circles) always treated a smaller volume. The Varian (2.5 mm) (red circles and stars) varied between treating the smallest and largest volume, e.g did not follow a clear trend.

For cases with 3 targets the distance between the targets had almost no influence on plans optimized with the same linac, with Varian (2.5 mm) (red) as an exception. Overall, Varian (2.5 mm) might seem to be the preferred linac-model for all cases, with 3 distant targets as an exception.

Treatment plans optimized with **single isocenter and treat** are shown in fig. 4.1.1(c). Overall, the quality treatment plans was improved. Almost all plans for cases with 2 targets fulfilled the V_{12Gy} -criteria. The impact of linac and/or location of targets was also reduced. Despite reduced difference in volume treated, when comparing treatment plans for the same case, Varian (2.5 mm) (red) treated 7-14.3% smaller volume compared to Elekta (5 mm gap). The treatment plan based on 3 distant GTVs showed the opposite trend. Here Varian (2.5 mm) (red circle) treated 8.5% more normal brain tissue. However, this plan did not fulfill the acceptable plan criteria and will be discussed later.

4.1.2 Brain dose, V_{3Gy}

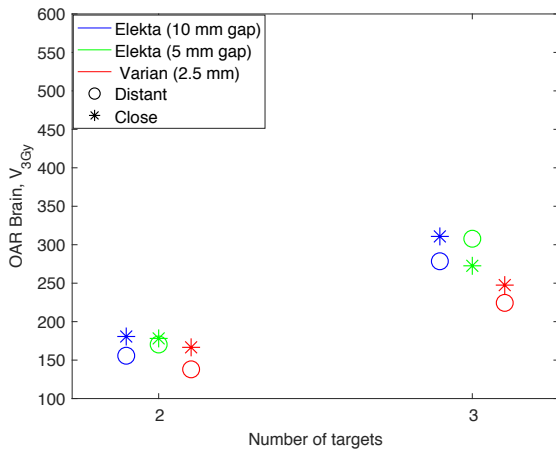
The impact of different linac-models for normal brain tissue (OAR Brain) treated with 3 Gy or more (V_{3Gy}) can be seen in fig. 4.1.2. The impact of different linac-models for treatment plans using **1 isocenter pr.target** as planning strategy is shown in fig.4.1.2(a). The size of V_{3Gy} showed about the sensitivity of location of GTVs for all linacs.

When comparing treatment plans based on the same case, Varian (2.5 mm) (red) treated the smallest volume, while Elekta (10 mm gap) (blue) and Elekta (5 mm gap) (green) varied between treating the largest volume. For cases with the same number of targets, almost all plans based on distant GTVs (circles), gave lower dose than the close GTVs (stars).

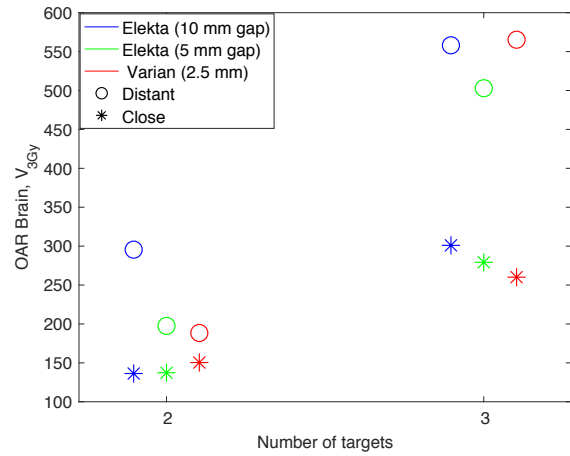
For treatment plans with **single isocenter** fig. 4.1.2(b) all treatment plans for the same number of targets treated a larger volume for distant GTVs (circles) than close GTVS (stars). The impact of distance between the targets were of most importance for cases with 3 targets. Compared to the other treatment plans that treated less than 350 cm^3 , these plans treated more than 500 cm^3 .

A common trend of the choice of linac-models was not clearly observed, but Elekta (5 mm gap) (green) showed good plan quality for most plans. These plans were also less influenced by location of GTVs. The treatment plans based close GTVs were less influenced of the linac-model.

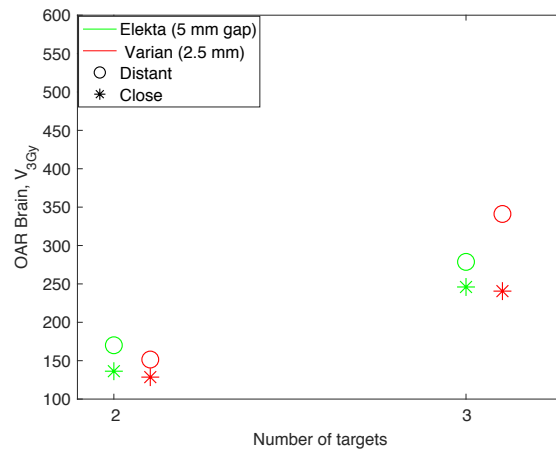
Treatment plans optimized for **single isocenter and treat** is shown in fig. 4.1.2(c). When comparing cases with the same number of targets, distant GTVs (circles) gave higher dose than cases with close GTVs (stars). Both linac-models showed about the same impact of location. Varian (2.5 mm) showed more sensitivity with respect to location for cases with 3 targets. However this plan was sub-optimal.



(a) 1 isocenter pr.target

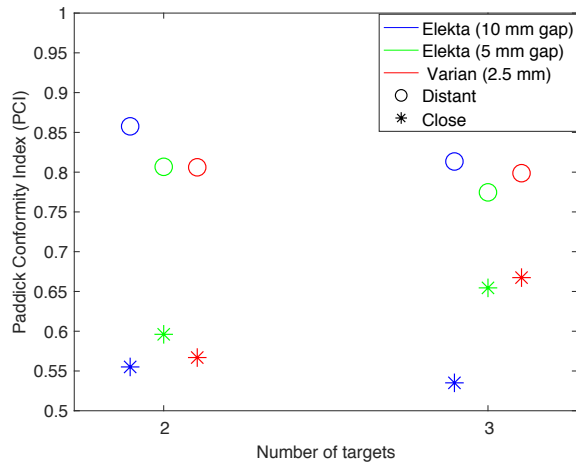


(b) Single isocenter

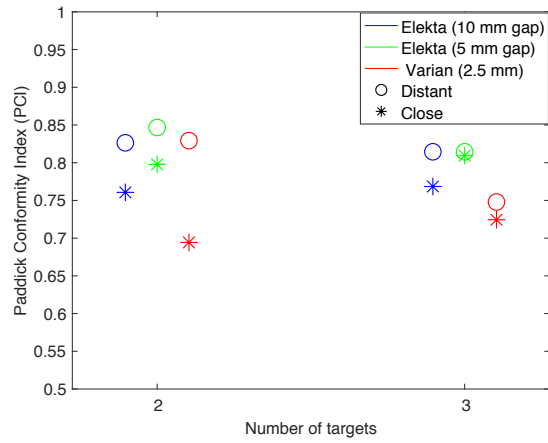


(c) Single isocenter and *treat*

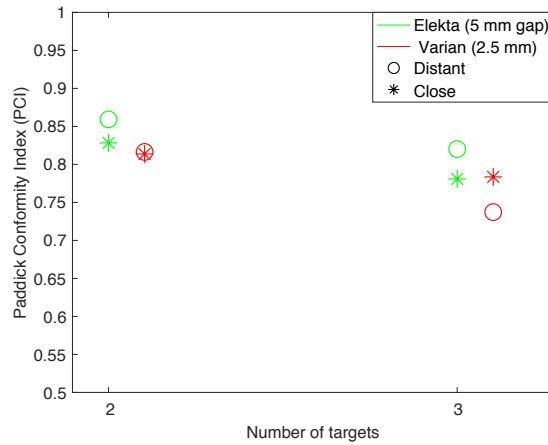
Figure 4.1.2: Volume[cm³] of normal brain tissue that receives 3 Gy or more for cases with different number of targets. Each sub-plot (a,b,c) shows the impact of different linac-models(represented with 3 different colours) for treatment plans optimized with the same treatment planning strategy. The plans were made for all cases, where circles represent cases (1 and 3) with distant GTVs, while stars show cases (2 and 4) with close GTVs.



(a) 1 isocenter pr.target



(b) Single isocenter



(c) Single isocenter and —textittreat

Figure 4.1.3: Paddick Conformity Index (PCI) for cases with different number of targets. Each sub-plot (a,b,c) shows the impact of different linac-models (represented with 3 different colours) for treatment plans optimized with the same treatment planning strategy. The plans were made for all cases, where circles represent cases (1 and 3) with distant GTVs, while stars show cases (2 and 4) with close GTVs.

4.1.3 Paddick Conformity Index

The impact of different linac-models for PCI can be seen in fig. 4.1.3. The PCI for all treatment plans were calculated from the eq. 2.4 for the union of PTV-volumes.

Treatment plans with **1 isocenter pr.target** is shown in fig. 4.1.3(a). All treatment plans with distant GTVs (circles) showed highest conformity, independent of linac used. Most treatment plans for distant GTVs had a PCI higher than 0.8. While the PCI of treatment plans for close GTVs was often lower than 0.6. The plans optimized with Elekta (10 mm gap) (blue) showed most sensitivity to the location of GTVs. This plans had highest PCI for distant GTVs (blue circles), and lowest PCI for close GTVs (blue stars). The plan for 3 close targets was not optimal with respect to the dose coverage of GTV, and will be discussed in detail later.

Treatment plans using **single isocenter** as planning strategy is shown in fig. 4.1.3(b). Overall, for plans based on the same number of targets, distant GTVs (circles) showed higher PCI than close GTVs (stars). In general, the impact of location on PCI was reduced when the number of targets increased. The plans optimized with Elekta (5 mm gap) (green) were less influenced by location of GTVs. When comparing the plans for each case, these plans also showed highest conformity. Varian (2.5 mm) showed low PCI for all treatment plans, with 2 distant GTVs as an exception.

Overall, the treatment plans optimized **single isocenter combined with treat**, shown in fig. 4.1.3(c), showed a high PCI, larger than 0.78, for almost all plans. Neither the linac nor the distance between the targets were of great importance for PCI. Elekta StO modified (green) showed highest PCI for all distant GTVs (circles), while the linac-models showed the same PCI for the close-cases (stars).

4.1.4 Dose Gradient Index

The impact of different linac-models for DGI can be seen in fig. 4.1.4. DGI for all treatment plans was calculated from eq. 2.5 for the union of PTVs. Most of the treatment plans showed a DGI between 0.2-0.3.

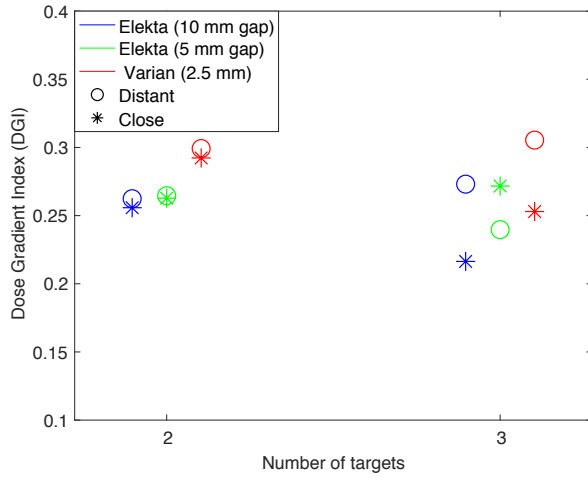
Overall, treatment plans using **1 isocenter pr.target** as planning strategy, seen in fig. 4.1.4(a), showed higher DGI for distant GTVs (circles) than close GTVs (stars) for treatment plans based on the same number of targets. However, the location of GTVs showed little impact on DGI, especially for cases with 2 targets. Here all plans using Varian (2.5 mm) had highest DGI. The plans for cases with 3 targets did not show a common trend with respect to location, nor linac.

Treatment plans optimized with **single isocenter**, shown in fig. 4.1.4(b), showed sharper fall off for close GTVs (stars) than distant GTVs (circles) for the same number of targets. Varian (2.5 mm) showed highest GTV for each case, with 3 distant GTVs an exception. Cases with 2 targets were influenced by the location of GTVs. The DGI for Elekta (10 mm gap) (blue circle) and Elekta (5 mm gap) (green) varied most with respect to location (difference between circle and star). For cases with 3 targets, Varian (2.5 mm) seemed to be most sensitive of distance between GTVs.

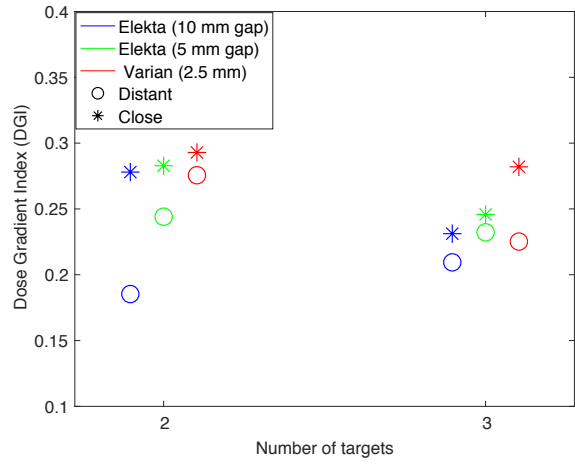
When using **single isocenter with treat** as treatment planning strategy, shown in fig. 4.1.4(c), plans for 2 targets optimized with the same linac-model showed little impact of the location of GTVs. All plans for Varian (2.5 mm) (red star and circle) showed sharper fall-offs than Elekta StO (5 mm gap) (green star and circle). Treatment plans for 3 targets, showed less impact of linac-model on DGI. However the impact of location increased. The plans for close GTVs showed higher DGI than the plans for distant GTVs.

4.2 Treatment planning strategies

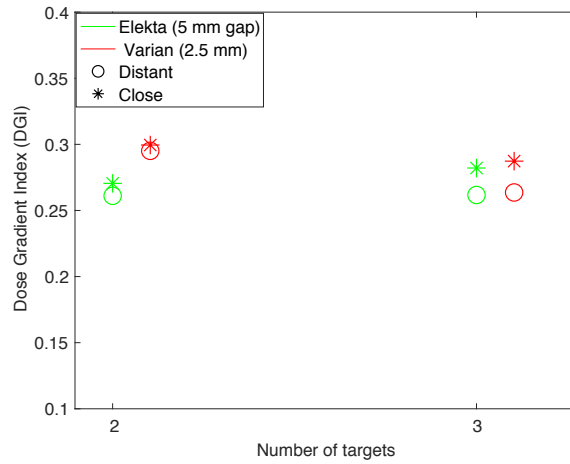
The following section compares treatment plans optimized by the same linac, but different treatment planning strategies: **1 isocenter pr.target**, **Single isocenter** and **Single isocenter and treat**. Important to note,



(a) 1 isocenter pr.target



(b) Single isocenter



(c) Single isocenter and treat

Figure 4.1.4: Dose Gradient Index (DGI) for cases with different number of targets. Each sub-plot(a,b,c) shows the impact of different linac-models (represented with 3 different colours) for treatment plans optimized with the same treatment planning strategy. The plans were made for all cases, where circles represent cases (1 and 3) with distant GTVs, while stars show cases (2 and 4) with close GTVs.

as mentioned in section 3.4, the *treat*-functionality did not work for Elekta (10 mm gap). 1 isocenter pr.target and single isocenter were the only treatment planning strategies for this linac-model.

4.2.1 Brain dose, V_{12Gy}

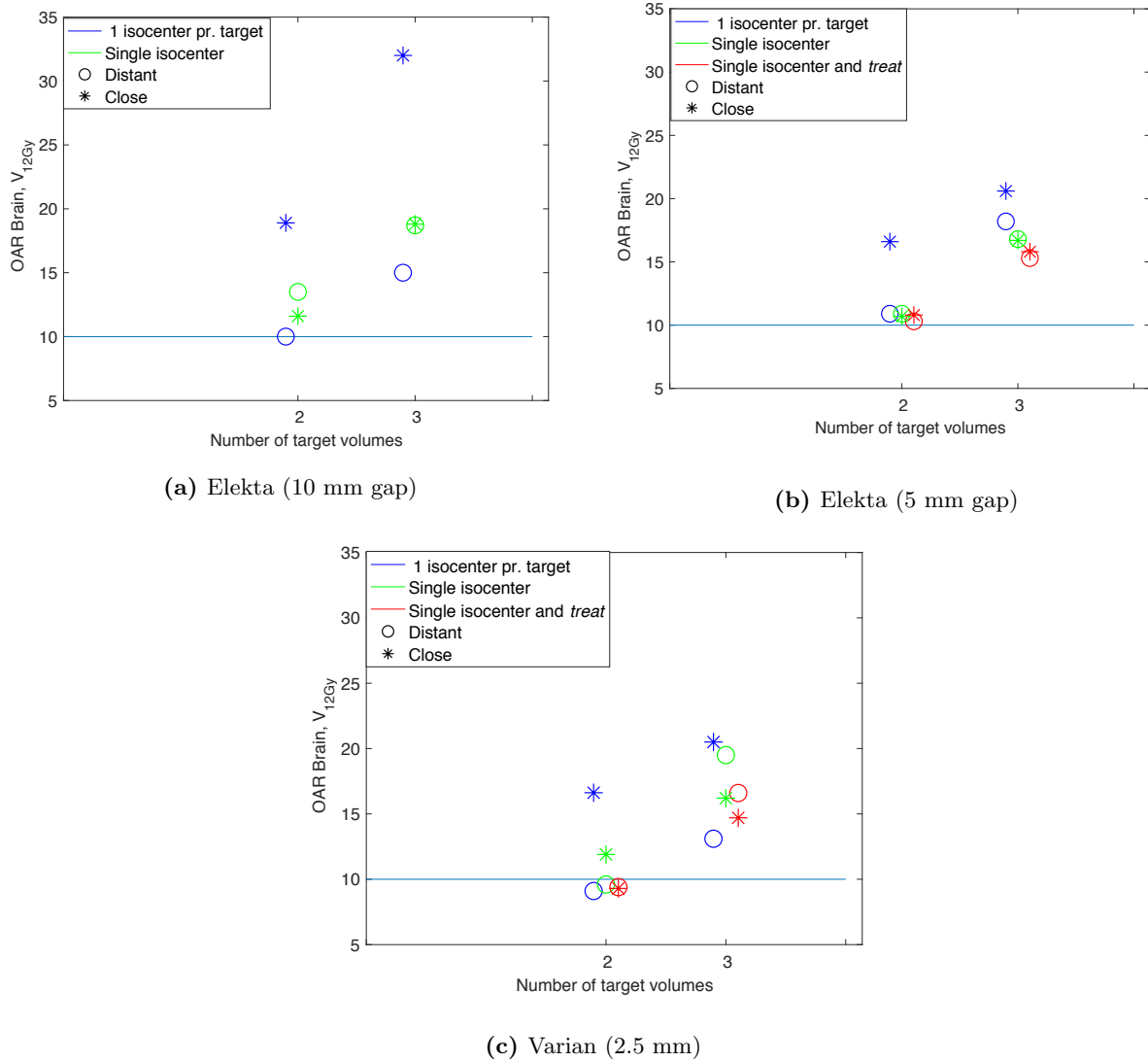


Figure 4.2.1: Volume [cm^3] of normal brain tissue that receives 12 Gy or more for cases with different number of targets. Each sub-plot (a,b,c) shows the impact of different treatment planning strategies (represented with 3 different colours) for treatment plans optimized with the same linac-model. The plans were made for all cases, where circles represent cases (1 and 3) with distant GTVs, while stars show cases (2 and 4) with close GTVs.

The impact of different treatment planning strategies for normal brain tissue (OAR Brain) treated with 12 Gy or more (V_{12Gy}) can be seen in fig. 4.2.1. As described in section 4.1.1, V_{12Gy} should not override 10 cm^3 . To study which treatment plans that fulfilled this criteria the limit is represented by a blue line in the plots.

The impact of different treatment planning strategies for treatment plans optimized with **Elekta (10 mm gap)** is shown in fig. 4.2.1 (a). Overall, V_{12Gy} for treatment plans optimized with 1 isocenter pr.target was highly influenced by location of GTVs. For plans based on distant GTVs 1 isocenter pr.target (blue circle) treated a small volume and was the favourable strategy. For plans based on close GTVs (blue star), this strategy treated a larger volume and was less favorable. This impact of location increased when the number of targets increased. For 2 targets V_{12Gy} increased with 88.9% for close GTVs compared to distant GTVs, while for 3 targets it increased with 113.4%. However, the plan for 3 close targets was sub-optimal e.g the plan criteria were not acceptable and will be discussed later.

When single isocenter (green star and circle) was chosen as planning strategy the location of GTVs did not seem to influence the size of V_{12Gy} in the same way. Most clearly observed for plans for cases with 3 targets where the the volume treated differed about 0.5%.

The treatment plans optimized with **Elekta (0.5 mm gap)**, shown in fig. 4.2.1(b), showed less impact of the treatment strategy with respect to location. Especially when studying cases with 2 targets, all plans, with 1 isocenter pr. target for close GTVs (blue star) as an exception, was located at almost same dose level. This plan treated more than 50% normal brain tissue. All the other plans for 2 targets had a V_{12Gy} under 11 cm^3 e.g were close to the V_{12Gy} -limit.

For cases with 3 targets, the treatment strategy were of more importance. The location of GTVs, however, showed little influence with respect to treatment strategy, e.g stars and circles of same colour were located close to each other. Overall, 1 isocenter pr.target (blue) treated the largest volume, while single isocenter combined with *treat* (red) seemed to be the most favourable strategy. For 3 close GTVs, 1 isocenter pr.target treated 23.2% more of normal brain tissue compared to the plan with *treat*.

Fig. 4.2.1(c) illustrates the impact of treatment strategy for plans optimized with **Varian (2.5 mm)**. The impact of location GTVs on treatment planning strategy was observed. For plans based on close GTVs (stars), single isocenter combined with *treat* (red) was the most favourable strategy, while 1 isocenter pr.target (blue) was least favourable. For treatment plans based on distant GTVs (circles) 1 isocenter pr.target (blue) was most favourable, while the single isocenter-plans (green) treated the largest volume. Overall, the treatment plans that combined single isocenter with *treat* (red circle and star) were less influenced by the location of GTVs. V_{12Gy} differed most for 3 targets. It increased with 12.9 % for distant GTVs compared to close GTVs.

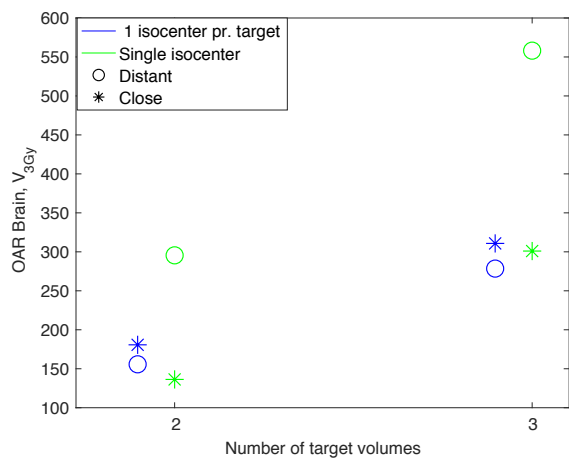
For 2 distant GTVs the choice of treatment planning strategy was of less importance. All these plans were below the V_{12Gy} -limit.

4.2.2 Brain dose, V_{3Gy}

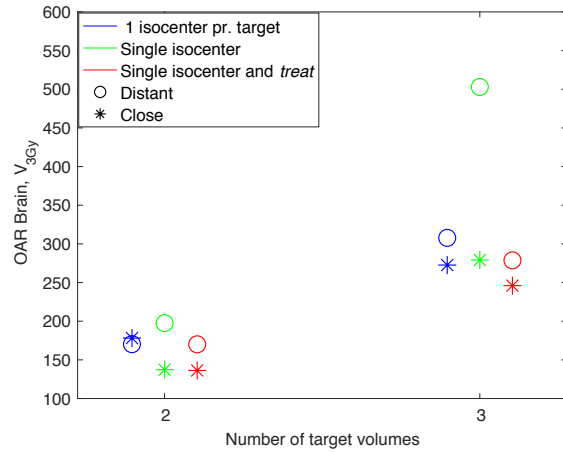
The impact of different treatment planning strategies for normal brain tissue (OAR Brain) treated with 3 Gy or more (V_{3Gy}) can be seen in fig. 4.2.2. The impact of treatment planning strategies for plans using **Elekta (10 mm gap)** is shown in (a). Treatment plans optimized with single isocenter (green) showed most impact of the location of GTVs. For close GTVs (stars) it seemed to be the favorable strategy, while the plans for distant GTVs (circles) were less favourable. When treating 3 distant targets, single isocenter was little favourable. The volume treated were larger than 500 cm^3 , in contrast to approximately 300 cm^3 for the other plans with 3 targets.

Treatment plans using 1 isocenter pr.target as planning strategy showed little impact of the location of GTVs. However, the strategy seemed to be a bit more favourable for distant GTVs.

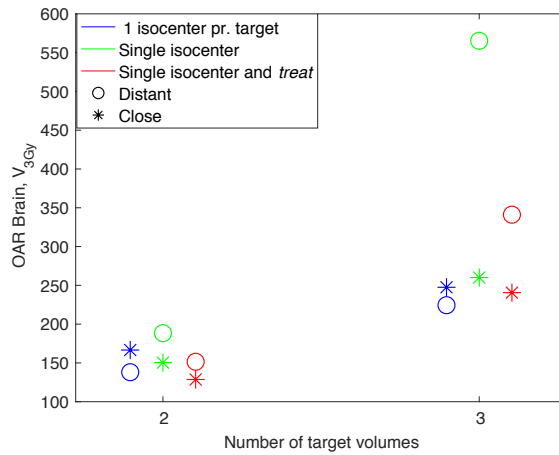
For treatment plans using **Elekta (5 mm gap)** the impact of different treatment planning strategies is shown fig. 4.2.2(b). Treatment plans based on 2 targets none of the treatment planning strategies were



(a) Elekta (10 mm gap)



(b) Elekta (5 mm gap)



(c) Varian (2.5 mm)

Figure 4.2.2: Volume[cm³] of normal brain tissue that receives 3 Gy or more for cases with different number of targets. Each sub-plot (a,b,c) shows the impact of different treatment planning strategies (represented with 3 different colours) for treatment plans optimized with the same linac-model. The plans were made for all cases, where circles represent cases (1 and 3) with distant GTVs, while stars show cases (2 and 4) with close GTVs.

very sensitive to the location of GTVs. The same trend was observed for plans with 3 targets, with single isocenter as an exception.

Almost all plans for close GTVs (stars) treated a smaller volume compared to the ones with distant GTVs (circles) for the same number of targets. For close GTVs, single isocenter combined with *treat* (red star) seemed to be the most favourable strategy, while the two others varied in order. For distant GTVs, single isocenter (green circle) treated the largest volume, while the other strategies varied between treating the smallest volume. As in **(a)** single isocenter- plans showed most impact of location for $V_{3\text{Gy}}$. This trend increased with the number of targets.

Treatment plans with different treatment planning strategy optimized for **Varian (2.5 mm)** are shown in fig. 4.2.2**(c)**. Overall, for cases with 2 targets, treatment planning strategy was little influenced by location of GTVs. For cases with 3 targets, single isocenter (green) and single isocenter and *treat* (red) were sensitive to location of GTVs. This was most clearly observed for single isocenter (green). The plan for distant GTVs (green circle) treated a volume larger than 550 cm^3 compared to about 300 cm^3 for other plans with the same number of targets. However, plan using single isocenter and *treat* has sub-optimal acceptance criteria and will be discussed later.

In general, the treatment planning strategies showed less impact for cases with close GTVs (stars) than for cases with distant GTVs (circles). 1 isocenter pr.target(blue) were the most favourable strategy for cases with distant GTVs (blue circles), while single isocenter (green circle) seemed to be the least favourable. For the plans based on close GTVs, single isocenter and *treat* (red stars) seemed to be the most favourable strategy.

4.2.3 Paddick Conformity Index

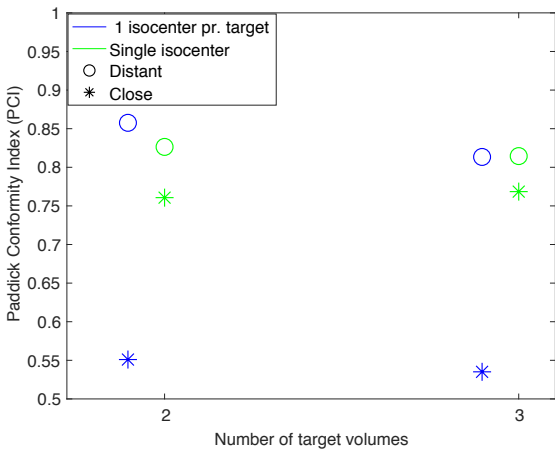
The impact of different treatment planning strategies for PCI can be seen in fig. 4.2.3. PCI was calculated from eq. 2.4 for the union of PTV-volumes.

For the treatment plans optimized with **Elekta (10 mm gap)**, shown in **(a)**, the number of targets showed less influence of the PCI. The location of GTVs was of most importance for plans optimized with 1 isocenter pr.target (blue). Treating close GTVs with 1 isocenter pr.target (blue stars) little favourable. The PCI of these plans was lower than 0.55, in contrast to about 0.8 for the other plans. For the treatment plans optimized with single isocenter (green) the location of GTVs was of less importance. Despite this, single isocenter seemed to be a more favourable strategy for close GTVs (stars) than distant GTVs (circles).

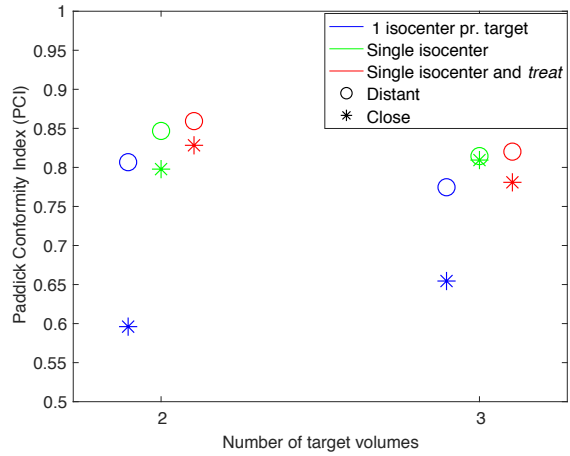
Elekta (5 mm gap) as linac-model, shown in fig. 4.2.3**(b)** generated more even treatment plans. The majority of plans were little influenced by treatment strategy or location of GTVs. Single isocenter combined with *treat* (red) was the most favourable strategy for all cases, with 3 close targets, as an exception. Treating close GTVs with 1 isocenter pr.target was little favourable, these treatment plans showed a PCI on the 0.6-level in contrast to a PCI higher than 0.8 almost all the other plans.

Treatment plans using **Varian (2.5 mm)** as linac-model, shown in fig. 4.2.3**(c)**, contributed to more variations between the plans compared. As for the other linac-models, the plans with 1 isocenter pr.target (blue) were influenced by location of GTVs. When treating close GTVs the PCI was low. Single isocenter (green) showed some sensitivity to location for cases with 2 targets. However, single isocenter with or without *treat* were little influenced by location of GTVs.

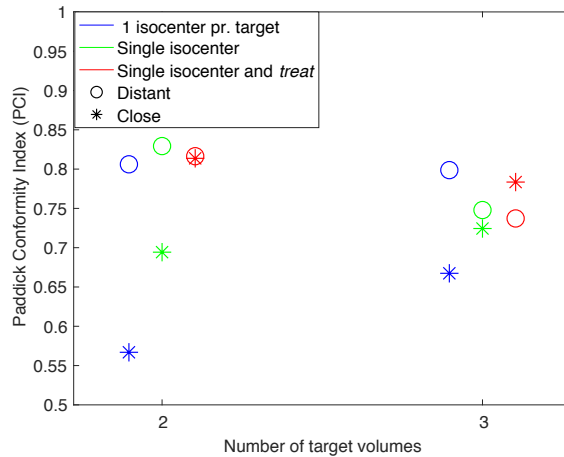
For plans based on close GTVs (stars) the treatment strategy influenced the PCI. Single isocenter and *treat* (red star) was the most favourable strategy, while 1 isocenter pr.target (blue star) seemed to be less favourable. For plans based on distant GTVs (circles) a clear trend was not observed.



(a) Elekta (10 mm gap)



(b) Elekta (5 mm gap)



(c) Varian (2.5 mm)

Figure 4.2.3: Paddick Conformity Index (PCI) for cases with different number of targets. Each sub-plot (a,b,c) shows the impact of different treatment planning strategies (represented with 3 different colours) for treatment plans optimized with the same linac-model. The plans were made for all cases, where circles represent cases (1 and 3) with distant GTVs, while stars show cases (2 and 4) with close GTVs.

4.2.4 Dose Gradient Index

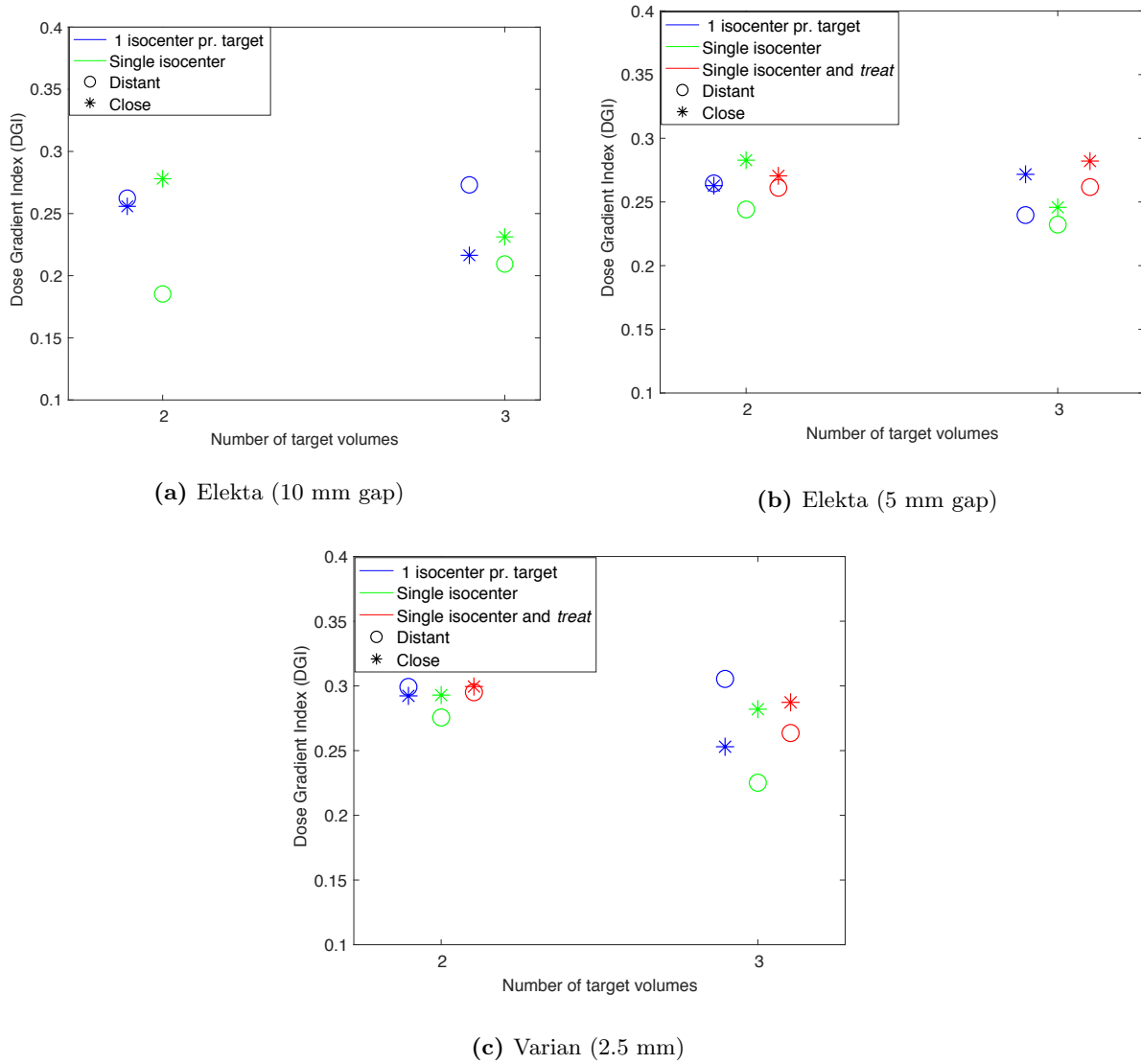


Figure 4.2.4: Dose Gradient Index (DGI) for cases with different number of targets. Each sub-plot (a,b,c) shows the impact of different treatment planning strategies (represented with 3 different colours) for treatment plans optimized with the same linac-model. The plans were made for all cases, where circles represent cases (1 and 3) with distant GTVs, while stars show cases (2 and 4) with close GTVs.

The impact of different treatment planning strategies for DGI can be seen in fig. 4.2.4. DGI was calculated from equation 2.5 for the union of PTVs. The DGI calculated in this study was between 0.2-0.3 for most treatment plans.

For treatment plans optimized with **Elekta (10 mm gap)**, shown in (a), using single isocenter for distant GTVs (green circle) seemed to be little favourable. For cases with 2 targets, the DGI for the other treatment plans were less influenced by location of GTVs or strategy used. All showed a DGI on the 0.3-level. The DGI for treatment plans based on 3 targets varied more. Using 1 isocenter pr.target for distant GTVs (blue circle) showed a DGI close to 0.3, while the other plans had lower DGIs.

When using **Elekta (5 mm gap)**, shown in fig. 4.2.4(b), the DGI was less dependent on the treatment strategy, number and location of targets. All plans had a DGI of 0.25 or higher. For plans based on 2 targets, location showed little impact for plans optimized by the same treatment planning strategy. The plans using single isocenter were more dependent on location. Overall 1 isocenter pr.target seemed to be the favourable strategy for plans with distant GTVs (blue circle), while single isocenter seemed to be the favourable strategy for close GTVs (green star).

For 3 targets the DGI differed more with respect to location. However, the DGI single isocenter with or without *treat* (green and red) was little influenced. Combining single isocenter with *treat* (red) showed sharpest fall off for both distant and close GTVs. For distant GTVs (circles), the two other planning strategies (blue and green) showed about the same DGI. While for close GTVs (stars) 1 single isocenter showed about the same DGI as *treat*.

For treatment plans optimized with **Varian (2.5 mm)**, shown in fig. 4.2.4(c), plans with 2 targets showed little impact on DGI with respect to treatment strategy or location. With single isocenter on distant GTV (green circle) as an exception, all plans were placed close to 0.3-level. For plans based on 3 targets, the DGI for each treatment planning strategy was influenced on the location of GTVs. However, the plans with single isocenter and *treat* (red star and circle) showed less influence of location. For distant GTVs (circles) 1 isocenter pr.target (blue) seemed to be the best strategy. For close GTVs (stars), single isocenter, with and without *treat* (red and green), showed the same DGI.

Chapter 5

Discussion

The following section compares the results/observations with other studies found in literature. Additionally, limitations and options of further research will be presented.

5.1 Linear accelerators/MLC-configuration

5.1.1 Brain dose, V_{12Gy} and V_{3Gy}

The impact of different linac-models for normal brain tissue (OAR Brain) treated with 12 Gy or more (V_{12Gy}) can be seen in fig. 4.1.1 Overall, Varian (2.5 mm) treated the smallest volume in most treatment plans. However, for treatment plans with close GTVs, Elekta (5 mm gap) treated about the same volume. Treatment plans optimized with Elekta (10 mm gap) showed most sensitivity to the location of GTVs. Especially when 1 isocenter pr.target was chosen as treatment planning strategy. Here V_{12Gy} was more than 55% higher for the treatment plan based on close GTVs, compared to the plan based on distant GTVs. The same sensitivity was observed for the two other linacs, but to a lower degree. Among them, Elekta (5 mm gap) was less influenced by location of GTVs.

However, V_{12Gy} is the predictor of risk of RN, even small differences in absolute volume treated might be of great importance. As an example, the linac-models showed less impact of treatment plans optimized with single isocenter and *treat*. Despite reduced difference in absolute volume treated, when comparing treatment plans for the same case, Varian (2.5 mm) (red) treated 7-14.3% (dependent on location of GTVs) smaller volume compared to Elekta (5 mm gap). The difference in % might be of more importance, and should be studied in more depth. Only treatment plans based on 2 targets treated a volume below 10 cm^3

The impact of different linac-models for normal brain tissue (OAR Brain) treated with 3 Gy or more (V_{3Gy}) can be seen in fig. 4.1.2. Overall, the treatment plans were more influenced of the linac model when the distance between and number of targets increased. Varian (2.5 mm) treated the smallest volume most often, with some plans based on distant GTVs as exceptions. In these cases the treatment plan optimized with Elekta (5 mm gap) treated a smaller volume. Overall, the linac-models showed the same sensitivity with respect to location for V_{3Gy} as for V_{12Gy} . However, two optimized treatment plans for the same linac-model, showed most variations in V_{3Gy} when single isocenter was chosen as treatment planning strategy.

A study done by Wu et al.[48] showed that using fine leaf of 2.5 mm in contrast to conventional 5 mm reduced the dose in radiosurgery treatment. Small targets with complex structure and/or location benefited the most. The treatment plans evaluated in this study were optimized IMRT or 3D-CRT. All metastases were either an integral part of or located close to critical structures. Another study of relevance, presented by Chae et al. [47], evaluated the effect of MLC leaf width for radiosurgery planning of spine lesions. The study compared the effect of leaf-width reduction for two modulated techniques, IMRT vs. VMAT. Decreasing

the leaf width resulted in improved target coverage, lower dose spillage and improved DGI. Using fine-leaf affected the quality of IMRT-plans more than the same plans using VMAT.

Based on the observations from this project leaf width of 2.5 mm and leaf tip gap smaller than 5 mm is favourable for the volume treated with different dose levels. Elekta (10 mm gap), could not utilize the *treat*-functionality in Raystation. The size of the tip-gap increased the flexibility of utilizing new functionalities in the treatment planning system. Overall, this linac-model varied more with respect to the others, especially when the treatment planning strategy was sub-optimal for the location of GTVs. Even though, Varian (2.5 mm) seemed favourable linac for most cases, Elekta (5 mm gap) showed stability with respect to location and treatment planning strategy. This might indicate that the dosimetric leaf gap rather than the leaf-width of MLC was of most importance.

5.1.2 Indexes, PCI and DGI

The impact of different linac-models for PCI can be seen in fig. 4.1.3. Overall, Elekta (5 mm gap) showed highest PCI for most treatment plans, while Varian (2.5 mm) often showed lowest PCI. PCI was often higher for treatment plans based on distant GTVs, independent of linac used. This was most clearly observed for treatment plans optimized with 1 isocenter pr. target. As mentioned PCI should be 1 to achieve conformal target coverage, but the plans with close GTVs was on the 0.55-level compared to above the 0.75-level for distant GTVs. The impact from Elekta (10 mm gap) on PCI was most dependent on location of GTVs. For distant GTVs the plans optimized with this linac-model showed highest conformity, while for close GTVs it gave the lowest PCI.

As mentioned, the study done by Chae et al. [47] showed that decreasing the leaf width resulted in improved target coverage. Based on the observations from this project, this was not the case.

The impact of different linac-models for DGI can be seen in fig. 4.1.4. Overall, the impact of location and linac increased with the number of targets. Varian (2.5 mm) showed sharpest fall-offs for most cases, independent of location of GTVs and treatment planning strategy. Treatment plans using Elekta (10 mm gap) showed lowest DGI most often. Additionally, these plans were most sensitive to the location of GTVs. All linac-models showed the same sensitivity when single isocenter was chosen as treatment planning strategy.

The study done by Chae et al. [47] showed that decreasing the leaf width resulted improved target coverage, consequently improved DGI. Based on the study presented by Chae et al. [47], the treatment plans using Varian TrueBeam STx was expected to achieve sharper fall-offs. The observations in this project were as expected in relation to this study.

Overall, as for brain dose, Elekta (10 mm gap) this linac-model varied more with respect to the others, especially when the treatment planning strategy was sub-optimal for the location of GTVs. Even though, Varian (2.5 mm) seemed favourable linac for many cases, Elekta (5 mm gap) showed the same level of DGI for many treatment plans. Additionally, it showed higher PCI for many treatment plans. This might indicate that the dosimetric leaf gap rather than the leaf-width of MLC was of most importance.

However the studies done by Wu et al [48] and Chae et al. [47] differed from the projected presented in this thesis in several ways. First, only treatment plans using VMAT was evaluated. The effects described for Chae et al. was most clearly seen for IMRT-plans of complex shaped targets . Second, none of cases studied in this project contain metastases located close to critical structures. Even though the study presented in this thesis differ from the study done by Wu et al in several factors some trends can be compared. Due to less complex cases and more robust modulated technique, VMAT, the effects in our study might have been reduced.

5.2 Treatment planning strategies

5.2.1 Brain dose, $V_{12\text{Gy}}$ and $V_{3\text{Gy}}$

The impact of different linac-models for normal brain tissue (OAR Brain) treated with 12 Gy or more ($V_{12\text{Gy}}$) can be seen in fig. 4.2.1. Overall, treatment plans with 1 isocenter pr.target were most sensitive to the location of GTVs. Treatment plans based on close GTVs treated a volume of Independent of linac-model, single isocenter and not least single isocenter combined with *treat* were little influenced by location. For treatment plans optimized with Elekta (5 mm gap) and Varian (2.5 mm), where the *treat*-functionality was available, it seemed to be the favourable strategy. As described for linac-models, the impact of the the different treatment planning strategies must be studied in more depth to state whether a strategy is more favourable than others, for cases with different number and location of targets. Despite small differences in volume treated, the consequence of a % change in $V_{12\text{Gy}}$ must be more critically examined.

The impact of different linac-models for normal brain tissue (OAR Brain) treated with 3 Gy or more ($V_{3\text{Gy}}$) can be seen in fig. 4.2.2. Overall, treatment plans with single isocenter and *treat* treated the smallest volume for almost all cases. The treatment planning strategy showed little impact of $V_{3\text{Gy}}$ when comparing cases with close GTVs and the same number of targets. When comparing cases with the same number of targets, but different location, single isocenter showed most variations in the volume treated. The sensitivity of location was most clearly observed when the number of targets increased. Compared to the other treatment plans for 3 GTVs, that treated less than 350 cm^3 , the plan for 3 distant GTVs showed a $V_{3\text{Gy}}$ above 500 cm^3 .

Traditionally VMAT-plans with multiple metastases is made with 1 isocenter pr.target. Recent studies done by Clark et al. [26][27] showed that treatment plans optimized with a single isocenter, the geometric midpoint of all metastases, showed about the same target coverage. Plans with several isocenters often lead to collimator leakage, higher dose to normal tissue and redundant delivery of MU. All these treatment plans were optimized with a TrueBeam STx linear accelerator from Varian Medical Systems. This linac was equipped with 120 MLC with leaf width of 2.5 mm in the central area of 8 cm, and leaf width of 5 mm in the outer region.

These studies indicated that the single isocenter approach may be a sufficient alternative to the multiple isocenter technique. Overall, the plans optimized in these studies were improved, by highly conformal dose distribution and not least reduced treatment time. The treatment time for treatment plans with multiple targets is roughly proportional to the number of targets treated. A typically time schedule is 20 min. The single isocenter approach reduces the treatment time, the duration of treatment is often set to 15 min. This improves the clinical efficiency, but accurate patient positioning become even more important. Especially for small metastases located distant to the isocenter.

As described in the studies above [26][27] single isocenter might be an attractive alternative approach to the multiple-isocenter techniques. However, for cases with GTVs located distant to each other, the location of isocenter might be unfavourable. Based on the observations in this project single isocenter seemed not to be the favourable strategy for 3 distant GTVs.

Different solutions were tried out to reduce the dose spillage of treatment plans with distant GTVs. The solutions tested in this project is described in detail in section 5.3.2. Even though the low dose-volume was reduced, it was still larger for single-isocenter plans compared to plans using other treatment planning strategies. To improve these plans further e.g reducing the dose leakage, other solutions/methods should have tested. Here, an interesting option is a study done by Wu et al. [49]. This method will be described in more detail in section 5.4.3.

However when the *treat*-functionality was combined with single isocenter it treated the smallest volume for almost all cases, independent of location and number of targets. It seemed to be the favourable treat-

ment planning strategy. Combined with the solutions listed above new functionalities in TPS can improve the drawbacks of single isocenter.

5.2.2 Indexes, PCI and DGI

As mentioned the study presented by Clark et al. [26] single isocenter plans showed about the same target coverage as treatment plans using multiple isocenter. The treatment strategy had little impact of PCI. It also showed that the dose conformity increased when the GTVs were located distant to each other. Based on this, the observations in the project presented in this thesis, were as expected.

However, the definition of the conformity index differed from the one used in this study. CI was calculated with V_{Rx}/V_{PTV} , where V_{Rx} is the volume of the prescription dose, and V_{PTV} the PTV volume. As described in section 2.3.4 this definition do not take undertreatment into consideration. To make sure that the isodose covers the target volume, the conformity index proposed by Paddick, eq. 2.4 [19] was used for this project. Even though the definitions differs, PCI-values calculated by Clark et al. might indicate a trend.

Another study, also presented by Clark et al. [27], also compared the differences between treatment plans using single isocenter or multiple isocenter. In contrast to the first study presented, the definition of PCI here was equivalent to the one used in this project, eq. 2.4 described in section 2.3.4. Clark et al. found a median PCI of 0.72 for all VMAT plans. Additionally, treatment plans using single isocenter showed the same conformity as treatment plans with multiple-isocenters. Treatment planning strategy showed little impact of PCI.

The impact of different treatment planning strategies on PCI can be seen in fig. 4.2.3. The PCI of the majority of treatment plans was above 0.75, on same level as the study done by Clark et al [27]. Some treatment plans had less conformal dose coverage. This was most clearly observed for the plans using 1 isocenter pr.target. As mentioned PCI should be 1 to achieve conformal target coverage, but the plans with close GTVs was on the 0.55-level compared to above the 0.75-level for distant GTVs. Some plans were approved with sub-optimal quality. As an example, the plan optimized with Elekta (10 mm gap) covered only 99.49% of the last GTV. The least optimal GTV coverage was observed for the treatment plan based on 2 close targets. After optimizing with Varian (2.5 mm) one of the GTVs was covered with 98.35% only. When single isocenter was combined with treat, all plans showed high PCI.

The acceptance criterias for a plan also influenced the PCI. In this project, mentioned in 3, 98% of PTV should be covered with at least 100% of the prescription isodose, while 100% of GTV should be covered with 150% of the prescription isodose. In the first study presented by Clark et al. [26] 99-100% of each PTV was covered with 100% of the prescription isodose. Such differences might influence the PCI. However, most of the treatment plans in this study showed about the same PCI as the study done by Clark et al [26].

As mentioned, the treatment plans presented in the studies done by Clark et al. were optimized with Varian TrueBeam STx, identical to one of the linac studied in this project. The conclusions stated in these projects might not be the same for other linac-models, with increased leaf width of MLC, as the Elekta-models studied in the project presented in this report. The treatment planning strategies showed most impact on PCI when Elekta (10 mm gap) was used as linac-model. Based on the discussion in the section above, 5.1, the impact of treatment planning strategies observed in this project might be as expected.

The same studies done by Clark et al. also reported that $DGI \leq 3$ represented an acceptable level of isodose. DGI-values for cases with more than 1 target have not been sufficiently described. However, calculating the DGI of a plan, not to each target, is an interesting parameter to evaluate plan quality. When ≤ 3 targets are located close to each other a so-called phenomena called dose bridging, 50% isodose lines, can be observed. Increased dose spillage will again lead to less favourable GI-values. In future studies the researchers [26] expected to observe greater DGI in cases with multiple targets, especially when located close

to each other.

For this project, the impact of different treatment planning strategies on the dose fall-off, illustrated as DGI, is described in section 4.2.4. DGI should ideally be 1. However a DGI of 1 is almost never found. To evaluate the quality of the treatment plans they should be compared with the DGI of the Clark-study [26][27]. In contrast, the DGI-values in this project was calculated with the inverse definition, $V_{100\%}/V_{50\%}$. To be comparable the DGI-values obtained should therefore be $\geq 1/3$.

The impact of different treatment planning strategies on DCI can be seen in fig. 4.2.4. When studying the plots of DGI most of the treatment plans had a DGI between 0.2 and 0.3. The DGI was lower compared to the study by Clark et al. However, the cases studied contained more than 1 target, 2 or 3, making the situations more complex. According to their definition of DGI the researches expected higher DGI for multiple metastases. With the definition used in this project, a lower DGI was expected when the number of metastases increased.

As expected the DGI was influenced by the number of targets. DGI was more dependent of treatment planning strategy and location of GTVs when the number of targets increased. Single isocenter as planning strategy for distant GTVs resulted in low DGI. This was most clearly seen for the plans optimized with Elekta (10 mm gap). However a clear trend with respect influence of location on treatment strategy could not be found. The expectations from Clark, treatment plans based on close GTVs show lower DGI, was not observed. Most of the plans for 2 targets, especially when optimized with Varian (2.5 mm), showed DGI comparable to Clark's study.

5.3 Workflow

Fulfilling the plan objectives for all combinations of treatment planning strategies and linacs was demanding in some cases. For some treatment plans, the struggle resulted in sub-optimal plan quality. These plans have been mentioned and partly discussed in the section above. Other plans, showed good quality in the end, but required often more time and testing to find an optimal solution. In the following section the challenges related to the different treatment planning strategies will be further discussed.

5.3.1 1 isocenter pr.target

As described in section 3.4.1 the plans optimized with 1 isocenter pr.target fulfilled the objectives listed in table 3.4.2 for the plan dose, but not necessarily for the sub-beamset. For the first target, however, the computed dose was based on that beam-set only e.g the plan dose and beam-set dose were the same. The dose computed for the second and third target was based on the background dose from the first, first and second beamset respectively. An illustration of the dependency is shown in fig. 3.4.1. A treatment plan was approved if the sub-beamset covered at least 98% of the respective PTV with 18 Gy. If possible, 100% of the respective GTV was covered with 21.4 Gy. For many plans, the GTV-objective was only fulfilled for the plan dose.

Additionally the max dose, $D_{2\%}$ to GTV should not be higher than 27 Gy. Treatment plans based on close GTVs were most challenging. To make sure that the max dose was below the limit, the GTV coverage was often reduced. Even though the GTV-coverage was 100% in the plan dose, balancing the max dose with dose coverage might be questionable. Treatments based on plan dose should treat all targets at the same day. As described [26][27] using multiple isocenters is time consuming. For some patients radiation therapy can be uncomfortable. Increased treatment time make interruptions of treatment more probable. Despite the effects of interrupted treatment seem unclear, sufficient GTV-coverage in the sub-beamset is important.

Generally, limiting the max dose was challenging. A set of possible solutions was tried out. First, the

dose contribution from a sub-beamset to other targets (not treated with that beamset) was controlled. For treatment plans with distant GTVs, the max dose to the other target(s) was limited to 1 Gy. For plans with close GTVs, setting 1 Gy as limit lead to unwanted exit and error-messages from TPS. The max dose objective was therefore increased to 4 Gy. This objective had low weight the first iterations, and was then increased when TPS had solved other objectives. Limiting the dose to other targets pushed more dose in the direction of the target treated. For treatment plans based on close GTVs, this gradient was a bit unfavourable. It lead to increased max dose for the target treated with that sub-beamset.

For 3 close GTVs using 1 isocenter pr.target was especially challenging. For these plans the max dose objective to the target treated with that sub-beamset was changed to 26 Gy. Then most of the treatment plans kept their max dose under the limit. But, as discussed above, this was at the cost of the GTV-coverage. For the first target this was not so problematic, but for the other targets the background dose from other beamsets create difficulties. As a consequence, the second, and not least the third target were not equally weighted as the first target in the optimization process. This was seen by studying the DVHs of the respective treatment plans. The curves for the different targets differed in both dose and steepness.

As described above, keeping the max dose below 27 Gy to all GTVs might be challenging. Especially when the targets are located close to each other. In this project the max dose is limited to 150% of the prescription dose. Despite the uncertainties related to radiation therapy must be taken into consideration, making 150% safer, the cells enclosed by GTV should be killed. Maybe a higher dose could have been tolerated in some cases, especially if it goes on the cost of target coverage. However the dose outside GTV/PTV must be critically examined.

5.3.2 Single isocenter

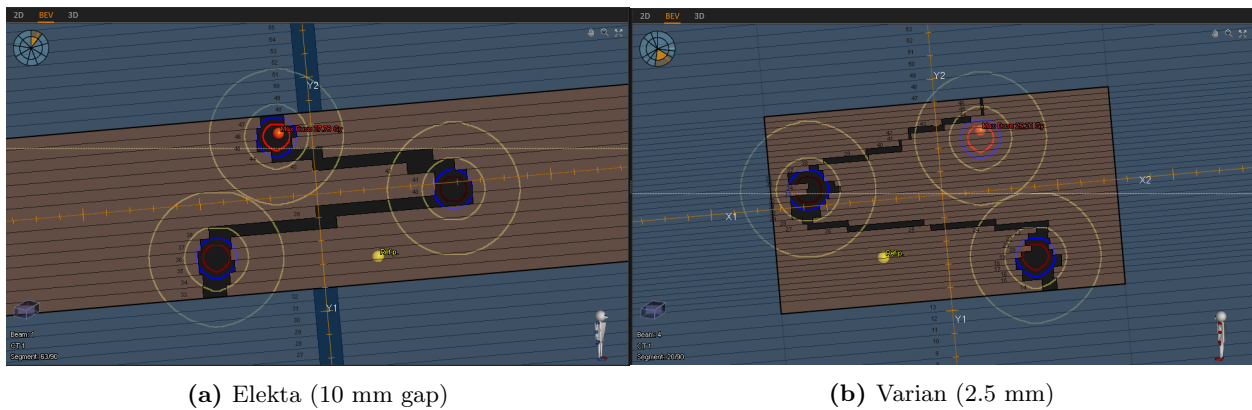


Figure 5.3.1: Case 3, 3 distant GTVs: The behaviour of MLC-leaves for different linac-models shown in BEV

In contrast to the treatment plans using multiple isocenters, located at the isocenter of each target, the plans using single isocenter were optimized for the geometric mid-point of the isocenters of all targets.

For multiple isocenter, the user/radiation-physicist had to go back and forth between the different sub-beamset and plan dose to make sure that all targets were almost equally weighted. Treating the second and/or third was highly dependent of the first target. For treatment plans optimized with single isocenter, all targets were visualized at the same time. Then it was easier to have an overview of the case. As described in section 3.4.2 the objectives listed in table 3.4.2 should be fulfilled for each target by the plan dose. Showing all objectives and doses simultaneously did not only lead to more equally weighted targets, but also shorter planning time.

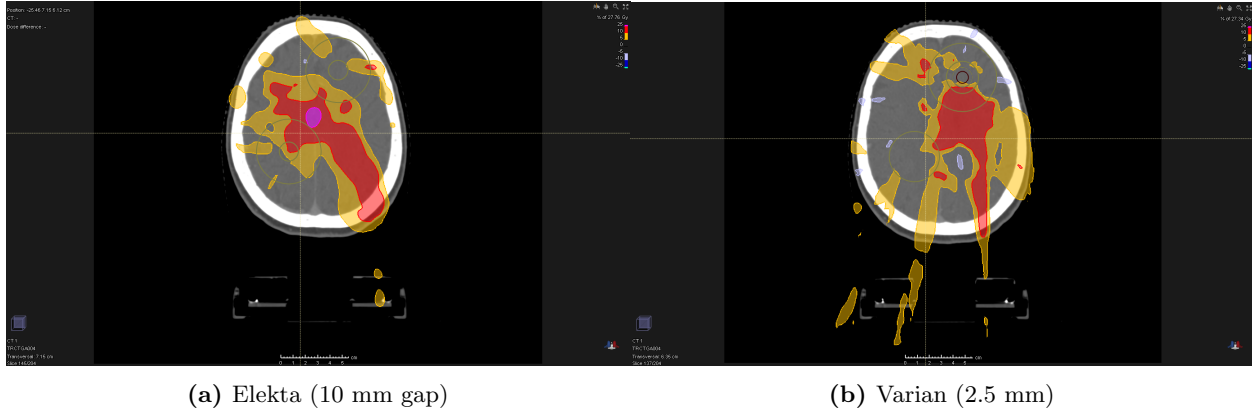


Figure 5.3.2: The effect of the brain-dose objective: Dose difference [%] between plans without and with the objective, in one CT-slice. The %-scale is illustrated with different colours, pink:25%, red:10% and yellow:5%.

However, as mentioned, the isocenter for these plans was the geometric midpoint between the targets. Even though the location of all targets was equally weighted, the isocenter-position was not always favourable for all targets. Based on the fact that the targets were not separated with the same distance, the location of isocenter matched some targets better than others. In general the distance to isocenter increased for cases with distant GTVs. However for 2 targets, the isocenter was located in the middle, being equally optimal/sub-optimal for both targets. For 3 targets, the location of isocenter was less favourable. The beam-eye-view(BEV) illustration of MLC-behaviour for case, shown fig.5.3.1, contributed to dose leakage between the targets. The single isocenter-plans were therefore highly influenced by the number and location of targets.

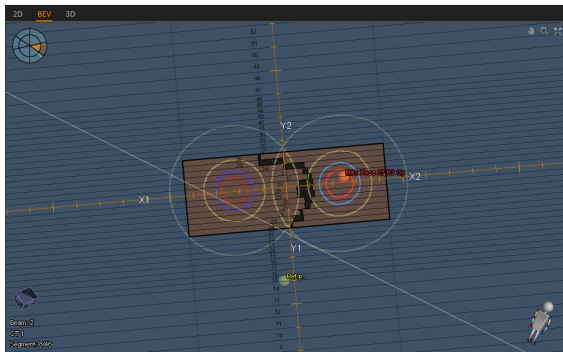
To improve the single isocenter-plans for 3 distant GTVs, an objective controlling the brain-dose was added. The low-dose contributed most to the dose leakage. The OARBrain should therefore not be higher than 4 Gy. The dose difference (for some CT-slices) between the plans without and with the brain dose-objective is shown in fig. 5.3.2. The low-dose spillage in the volume between the targets was reduced. This objective showed most effect for the treatment plans using Elekta (10 mm gap) (shown to the left), compared to Varian (2.5 mm) (shown to the right). The brain-dose to 2 distant GTVs was not controlled. These plans could probably be improved by setting a criteria controlling the brain-dose. However, the limit should be lower than 4 Gy since the dose leakage was less for this case.

Based on the discussion above, single isocenter as planning strategy was not only favourable in the planning process, but also in the treatments. Several studies have shown that single isocenter reduces the treatment time [26][27][49]. In contrast, the treatment time for multiple isocenters is proportional to the number of targets treated, leading to prolonged time in cases with many targets. Shorter treatment time do not only improve the clinical efficiency, but also lead to more comfortable treatment. This reduces the probability of exit. However an accurate patient positioning is of even more importance.

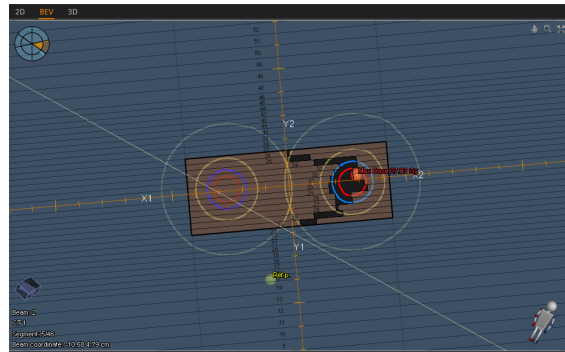
5.3.3 Single isocenter and *treat*

The MLC-behaviour for different treatment plans in BEV is shown in BEV in fig. 5.3.3. The upper row shows a possible scenario of MLC-behaviour for plans optimized with single isocenter. For these treatment plans TPS decided which beams that treated the different targets. When an arc changed which target to treat and moved between two targets situations leading to dose leakage was observed.

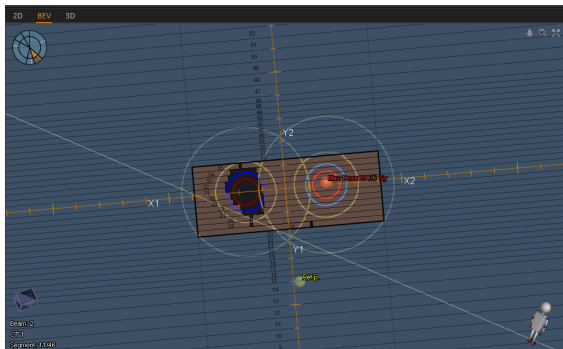
The lower row of fig. 5.3.3 shows plans that combined single isocenter with *treat*. In contrast, which beams that treated the different targets were strictly controlled. Even though some dose leakage was observed for these treatment plans, the MLC-opening follows the targets treated. Situations where arcs changed which



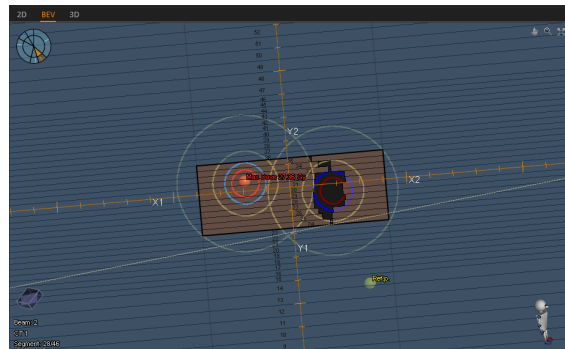
(a) Single isocenter



(b) Single isocenter



(c) Single isocenter with *treat*



(d) Single isocenter with *treat*

Figure 5.3.3: Upper row: MLC-behaviour for treatment plans using single isocenter. Lower row: MLC-behaviour for treatment plans using single isocenter with *treat*. All treatment plans were optimized with Varian (2.5 mm)

target to treat and moved between the targets were less probable.

As for single isocenter, the treatment plans were only evaluated by the plan dose. Then the targets were more equally treated. However, compared to the same case and linac with single isocenter, the DVHs for different targets in these treatment plans were extremely even.

However, in the beginning, almost all plans, independent of case and linac-model, lead to error-messages and unwanted exits. The *treat* function worked partly in the same way, contributed to the same effect, as the ring-objectives. Compared to treatment plans optimized with the other treatment planning strategies, the weight of the ring-objectives was very low. Decreasing the weight of the ring-objective was of most importance for Ring 2, ranging 0.5-2 cm outside PTV. However, low weight did always solve the programming error. None of the treatment plans using Elekta (10 mm gap) could handle the *treat*-functionality. Based on the fact that the *treat*-function controls the behaviour of MLC, how close the individual leaves can move to the PTV *treated*. The tip gap for this linac was 10 mm, then a margin of 0.4 cm was probably too small, not possible for the MLC-leaves.

For the two other linac-models the size of the margin could be challenging. In such situations, the error messages often told that one or more of the beams were problematic. Increasing the margins to 0.5 cm in the moving-direction of MLC-leaves for the respective beam(s) solved the problem. However, for an accurate comparison, the y-margins for all beams should be the same, 0.4 cm in the moving-direction of MLC.

As for single isocenter treatment plans for 3 distant GTVs were challenging. Also here, the brain-dose objective was added in hope to improve the plan. However, the brain-dose object showed less effect for these plans. For some reason, the treatment plan for Varian (2.5 mm) could not handle the objective. All solutions mentioned above were tested out, but it resulted in programming error only. This plan was optimized without the brain-dose objective and showed sub-optimal quality for all parameters evaluated in this study.

As mentioned in section 3.4.3 the beams were restricted to treat one target only. The first three beams treated the first target, then the next three beams treated the second target etc. In some situations, seen from BEV, the targets or ring structures shared the same plan or crossed each other. In these situations, treating several targets by the same arc could have been interesting option.

Despite, the start-up problems with the *treat*-function, it created better treatment plans in a shorter time. Additionally, since it partly replaced the effect of the ring-structures, it required less time from the user. The treatment plans using *treat* showed good score for all parameters evaluated in this project. Additionally the targets were equally treated. Consequently, optimizing treatment plans with *treat* was an easier, faster and better planning strategy.

5.4 Limitations/Future Work

5.4.1 Cases and delineation

The cases studied could have been more complex with respect to location and shape. All metastases were spheres with the same volume. Additionally, none of the metastases were located close to critical structures. As discussed in section 5.1 the impact of fine-leaf MLC increased for more complex cases. The same effect was also observed when treatment planning strategies were compared. Consequently, the impact of linac or treatment planning strategy might be of more importance than observed in this project.

In SRT a high dose is delivered in 1 or a few fractions. The high dose rate requires precisely control of dose delivery in order to limit the dose to normal tissue. The size of PTV depends on the accuracy in each steps of the treatment chain. Among the factors: accuracy of MRI, image registration, extension of tumor cells, accuracy in imaging, positioning and guiding during treatment. A study done by Kirkpatrick et

al. [28] tried to find an optimal margin for stereotactic radiosurgery (SRS). Their study compared margins of 1 and 3 mm. The volume receiving 12 Gy or more ($V_{12\text{Gy}}$) was higher in treatment plans with 3 mm. However, low local recurrence rate and RN was observed for both margins.

Even though a GTV expansion of 1 mm was the preferred choice, the 3 mm was chosen to account for the uncertainties in linac-based SRT [28][46]. However, a smaller margin could have improved the treatment plan.

In addition to the margin making PTV, two ring structures were made to control the dose fall off outside the target. For cases where the GTVs were located distant from each other the rings were controlled separately. In the optimization they were balanced with target coverage and max dose. The rings were tried to be equally weighted, but often one target was easier covered than the other(s). Then controlling the weight of the individual ring structures to each GTV was important.

For the other cases, close GTVs, the ring structures from different GTVs overlapped. To avoid volume with competing criteria e.g wanting high dose with respect to one target and low dose with respect to another, the dose fall off was controlled by the union of the ring structures. As mentioned above it might be favourable to control the dose fall-off of each target separately.

As an example, case 4 is characterized as a case with 3 close targets. In fact only two of the GTVs were located close to each other, but the ring-structures was controlled as a union of the three independent rings. As an alternative, maybe only two of the GTVs, here GTV_2 and GTV_3 , should be controlled with a union of the structures. The structures around GTV_1 were only overlapping in some slices, and ring 1 was never overlapping with the same rings from the other GTVs. Situations like that might be solved with dividing the ring structures in the middle.

However, when comparing the DVH of the union-ring with the DVHs of individual rings, they have not been equally pushed. Often some of the ring structures have been more pushed than the others. Even though the weight is increased for the union of the ring-structures, TPS seeks to find the optimal solution leading to more pressure in some directions than others.

However, utilizing new functionalities in the TPS, like the *treat*-function used here partly replace the ring-structures. The treatment plans using *treat* also showed very even DVHs for the different targets. However, the effect of the *treat*-functionality must be studied in more detail for more complex cases. Here other margins and structures might be more favorable.

5.4.2 Radiation equipment

Historically Gamma Knife (GK) has been superior to other SRT-techniques with respect to normal tissue exposure. They utilize a range of treatment techniques like high definition multi-leaf collimator (HD-MLC) and high intensity flattening filter free (FFF) beams. Combined with being capable and flexible using different planning strategies linac-based SRS has become competing with GK [32][33][27].

A study done by Thomas et al. [31] tried to investigate whether linac-based SRS plans using multi non-coplanar arcs VMAT could achieve the same quality as plans using GK. They found that the VMAT- plans improved the conformity, additionally no significant difference was observed in dose-fall, low isodose spillage or 12 Gy isodose volume. Additionally these plans showed a significant reduction in treatment time.

The cases studied in this project were not optimized with GK. However, the studies mentioned above showed that linac-based SRS gave acceptable plan quality. Despite increased flexibility in target chaping, the impact of different treatment techniques and components should be studied in more depth.

As described in section 2.1.2, FFF is favourable for SRT for several reasons. At first removing a filter reduces the head scatter. FFF-beams contribute to conformal shaping of the target e.g lower dose outside field edge and max dose in the middle of the target. And of great importance, due to higher dose rate the treatment time is reduced.

The plans with sub-beamset for every target, 1 isocenter pr.target, were optimized on the isocenter of each target. But the plans using single isocenter were optimized of the geometric midpoint of all targets. Then all, some more than others, were located distant to the isocenter. The profile of FFF-beams is shown in fig. 2.1.2 Despite the advantageous time-sparing of FFF-beams, the dose profile of the edges is less favourable for these targets.

However, VMAT is a very flexible technique in conformally shaping the targets through varying the the speed of gantry rotation, the configuration of MLC-leaves and the speed of gantry rotation [50]. It might smoothen it out. However, if single isocenter replaces the multi-isocenter technique for distant GTVs, the shape of the edges of FFF-beams should be studied in more depth.

5.4.3 Treatment planning system

As discussed in different studies by Clark et al. [26], using single isocenter was an attractive alternative to multiple-isocenter. However, as discussed in section 4.2.4c, the size of the low dose volume increased. For some cases, the isocenter became sub-optimal, leading to at worst 46% [51] more dose. As discussed in section ?? the same trends were observed in the project presented in this thesis. As described in section 5.3.2 the dose spillage was reduced by adding objectives in TPS. However, single isocenter seemed still not be favorable for distant GTVs.

In order to replace the multiple-isocenters with single isocenter, due to its increased clinical efficiency, many studies have tried to solve the drawback of dose spillage. A study done Wu et al. [49], proposed an algorithm called the Projection summing algorithm. Here, a multiplication of three matrices describing couch, collimator and gantry, projected the BEV-openings for different angles. In order to minimize the dose spillage the angles that resulted in the smallest openings were combined. Treatment plans that used this algorithm showed a significant reduction in the mean and low dose to the normal brain, while at the same time maintaining about the same treatment quality. The cases studied had 3 - 5 metastases, and based on these results single isocenter is an attractive approach treating multiple metastases.

For the projected presented here, the number and directions of arcs in this were chosen according to the procedure at St.Olavs, independent of location and number of targets. Based on the results from Wu et al. [49] choosing appropriate angles and number of arcs reduces the dose spillage. The treatment plans presented in this report should have been tested with more appropriate combinations of angles. In future studies, with more complex cases, with respect to location and number of targets, case-specific angle-combination might be of even more importance. The algorithm was integrated to Eclipse treatment planning system. Even the treatment plans in this thesis was supported by another software program, Raystation, a similar approach should be possible.

5.4.4 Radiobiology/risk analysis

Despite the risk of RN after SRT depends on a variety of factors: radiation techniques, type of lesion, patient selection etc. some good predictors have been found. Together with V_{12Gy} , V_{10Gy} , have been shown to be relevant volumes in evaluating the risk RN. Several studies done by Blonigen et al. [34] described how the volume treated with different dose levels affected the survival of patients. They found that V_{12Gy} larger than 10.8 cm^3 and V_{10Gy} larger than 14.5 cm^3 showed a risk for RN up to 68.8% [29]. Additionally, in order to minimize the risk of symptomatic radio necrosis another fractionations scheme was considered. V_{12Gy} larger than 7.9 cm^3 and V_{10Gy} larger than 10.5 cm^3 should rather be treated with several large fractions, $9\text{ Gy} \times 3$.

The project described in this thesis evaluated the volume treated with 12 Gy only. To avoid the risk RN, this volume should be limited, here 10 cm^3 . As described in chapter 4, in subsections 4.1.1 and 4.2.1, only a few of the treatment plans showed $V_{12\text{Gy}}$ below that size. The dose for all treatment plans were delivered in a single fraction. Based on the studies mentioned above, another schedule could have been more favourable for most cases.

5.4.5 Verification

The results discussed in this project were only computed in TPS. To check whether the same plan quality can be achieved for real patients, a quality assurance/verification-procedure with Delta4-phantom should be done. Different methods is used to make an estimates of deviation between the planned and measured dose. A number of pass/fail-criteria must be fulfilled for a treatment plan to be accepted.

The treatment plans in this study used small field sizes. Exact measurements of the dose distributions for these fields is challenging for linac-model in TPS and not least in verification. An example, as discussed in section 5.4.2, the dose profile for FFF-beams might be unfavourable for treatment plans using single isocenter for distant GTVs. To compensate for this, the treatment plans in TPS might be very complex, and probably difficult to measure and then verify.

Chapter 6

Conclusion

The aim of this study was to investigate the influence of different linear accelerator models and treatment planning strategies on irradiated volume of brain normal tissue (V_{12Gy} and V_{3Gy}), conformity and gradient index. The sensitivity for the location and number of GTVs was also studied.

Treatment plans for different linac-models and treatment planning strategies were made for 4 different multi-target brain cases. These plans were supported by the software RayStation (RaySearch Laboratories AB, v.5.99.0.5 Research). All plans were optimized with the same planning objectives, with some individual corrections for some cases, until they reached the same acceptable plan criterias.

Reducing the leaf width of MLC reduced the V_{12Gy} , V_{3Gy} , and increased the dose gradient. However, the conformity was reduced. Reducing the tip gap, for 5 mm leaf width, showed about the same impact on the volumes treated. The PCI for these plans The linac at St.Olavs, Elekta Versa HD Agility, was often the least favourable.

Single isocenter, especially when combined with new-functionalities in Raystation, showed less sensitivity to location of targets on V_{12Gy} . 1 isocenter pr.target treated a small volume for distant GTVs, but were less favourable for close GTVs. The same sensitivity for location was seen PCI. Overall, the PCI for most treatment plans was higher than 0.75. For 1 isocenter pr.target on close GTVs PCI was lower than 0.55. The DGI was 0.2-0.3 for most plans, with some single isocenter plans as exceptions. Single isocenter treated a large V_{3Gy} , compared to the other treatment planning strategies for distant GTVs.

Based on the result of this project, decreasing the leaf width and leaf tip gap improves the flexibility of the linacs. Due to low PCI for the plans using-fine leaf, the leaf tip gap, rather than the leaf width might be of most importance. Overall, the reduced flexibility of the linac at St.Olavs, Elekta Versa HD Agility, resulted in increased dose to normal tissue. This linac-model varied more with respect to the others, especially when the treatment planning strategy was sub-optimal for the location of GTVs. Compared with the plan optimized with close GTVs, the plan for distant GTVs treated a 55% larger V_{12Gy} .

Due to its size of tip gap, it could not utilize the new *treat*-functionality in Raystation. Despite some start up problems, the treatment plans optimized with the *treat*-function seemed to be created faster, better and less-user dependent treatment plans.

Single isocenter might be an attractive and time-effective alternative to the multiple-isocenter technique, especially when combined with new functionalities in the treatment planning system. However, when used for targets located distant to the isocenter, different methods should be tested in hope to reduce the dose spillage. Despite, utilizing new functionalities in the treatment planning system reduced the leakage, other solutions and algorithm should be tested and integrated. Especially, for more complex cases a more advanced

method is probably needed. Single isocenter showed most impact of DGI, and should also be evaluated in the different solutions.

The cases studied in this project lacked in complexity with respect to location and number of targets. The next step will be studies of cases located close to or as integral parts of a critical organ. In such cases, the observations done in this project might not only increase, but also be of more importance. Here even small differences in the absolute volume of V_{12Gy} , larger %-differences, could be of importance for the risk of RN. Other fraction schemes might be favourable for some cases.

However, the aim with the project presented in this report was to study the impact of different variables. To reduce the number of factors that contribute to the observed results, the complexity, a simple case would be an ideal starting point. The next step will be to study whether the trends observed here will be the same for more complex cases e.g higher number of targets located nearby critical structures.

Bibliography

- [1] P. Mayles, A. E. Nahum, and J-C Rosenwald, *Handbook of Radiotherapy Physics: Theory and Practice*. Boca Raton, FL, USA: Taylor Francis, 2007.
- [2] Laboratories, R., 2012c. Raystation 4.5, user manual.
- [3] C. Hægeland. *Optimization and verification of dosimetric robustness of VMAT dose-plans*. 2016, pp. 3-30
- [4] C. X Yu. "Intensity-modulated arc therapy with dynamic multileaf collimation: An alternative to tomotherapy". *Physics in Medicine and Biology*, 1995, Vol.40(9), pp.1435-1449
- [5] C.M Thompson, S.J Weston, V.C Cosgrove et al. "A dosimetric characterization of a novel linear accelerator collimator". *Medical Physics*, March 2014, Vol.41(3)
- [6] V. Gjervan. *VMAT for small cell lung cancer*. Master thesis, Norwegian University of Science and Technology, Faculty of Natural Sciences and Technology, Department of Physics, (2015), pp. 3-26
- [7] E. B. Podgorsak. *Radiation Oncology Physics: A Handbook for Teachers and Students*. Vienna, Austria: International Atomic Energy Agency, 2005.
- [8] J.S.Lilley. *Nuclear Physics, Principles and Applications*. The University of Manchester: Department of Physics and Astronomy, 2001
- [9] E.J. Hall, A J.Giaccia. *Radiobiology for the Radiologist*. Seventh Edition, Wolters Kluwer Health, Lippincott Williams and Wilkins, 2012
- [10] P. M. DesRosiers et al. "Lung cancer radiation therapy: Monte Carlo investigation of "under dose" by high energy photons". *Technology in cancer research treatment* 3.3 (2004), pp. 289–294.
- [11] K.E. Ekstrand and W. H. Barnes. "Pitfalls in the use of high energy X rays to treat tumors in the lung". *International Journal of Radiation Oncology* Biology* Physics* 18.1 (1990), pp. 249–252.
- [12] R.O. Kornelsen and M.E.J. Young. "Changes in the dose-profile of a 10 MV x-ray beam within and beyond low density material". *Medical Physics* 9.1 (1982), pp. 114–116.
- [13] M.E.J. Young and R.O. Kornelsen. "Dose corrections for low-density tissue inhomogeneities and air channels for 10-MV x rays". *Medical Physics* 10.4 (1983), pp. 450–455.
- [14] S. Levernes. *Volum og doser i ekstern stråleterapi - Definisjoner og anbefalinger. StrålevernRapport 2012:9*. Østerås, Norway: Statens strålevern (NRPA), 2012.
- [15] "ICRU Report 83: Prescribing, Recording, and Reporting Photon-Beam Intensity-Modulated Radiation Therapy (IMRT)". *Journal of the ICRU* 10.1 (2010).
- [16] C. X. Yu. "Intensity-modulated arc therapy with dynamic multileaf collimation: an alternative to tomotherapy". *Physics in Medicine and Biology* 40.9 (1995), p. 1435.
- [17] Norsk Lunge Cancer Gruppe og KVIST-gruppen. *Faglige anbefalinger for strålebehandling ved ikke-småcellet lungecancer*. July 2014.
- [18] J. Seuntjens, E. F. Lartigau, S. Cora et al. "PRESCRIBING, RECORDING, AND REPORTING OF STEREOTACTIC TREATMENTS WITH SMALL PHOTON BEAMS", *Journal of the ICRU*, 2014, Vol.14(2), pp.
- [19] I. Paddick, "A simple scoring ratio to index the conformity of radiosurgical treatment plans". Technical note, *J. Neurosurg*, 2000, Vol.93, pp. 219–222.
- [20] Kim, M.S, Kim, W.,Park, I.H. et al "Radiobiological mechanisms of stereotactic body radiation therapy and stereotactic radiation surgery". *Radiation Oncology Journal*, December 2015, Vol.33(4), pp.265-275

- [21] C. Song, M-S Kim, L. Cho et al. "Radiobiological basis of SBRT and SRS" *International Journal of Clinical Oncology*, Aug 2014, Vol.19(4), pp.570-8
- [22] R. Merwin, G.H Algire, H.S Kaplan "Transparent-chamber observations of the response of a transplantable mouse mammary tumor to local roentgen irradiation". *J Natl Cancer Inst.* Vol.19(11) pp.593-627
- [23] "Radiotherapy treatment planning: Benefits of CT-MR image registration and fusion in tumor volume delineation" D. Igor, P. Borislava, E. Marko Nikolić et al. "Radiotherapy treatment planning: Benefits of CT-MR image registration and fusion in tumor volume delineation". *Vojnosanitetski Pregled*, January 2013, Vol.70(8), pp.735-739
- [24] P. K Bagri, A. Kapoor, D. Singh, et al." Addition of magnetic resonance imaging to computed tomography-based three-dimensional conformal radiotherapy planning for postoperative treatment of astrocytomas: Changes in tumor volume and isocenter shift". *South Asian Journal of Cancer*, January 2015, Vol.4(1), pp.18-20
- [25] Y. R Lawrence, "Radiation Dose-Volume Effects in the Brain". *International Journal of Radiation Oncology, Biology and Physics*, 2010, Vol.76(3)
- [26] G. M. Clark, R. A. Popple, M. P. Brendan et al. "Plan quality and treatment planning technique for single isocenter cranial radiosurgery with volumetric modulated arc therapy". *Practical Radiation Oncology* Vol.2(4), 2012, pp. 306-313
- [27] G. M Clark, "Feasibility of Single-Isocenter Volumetric Modulated Arc Radiosurgery for Treatment of Multiple Brain Metastases". *International Journal of Radiation Oncology, Biology and Physics*, 2010, Vol.76(1)
- [28] J. P Kirkpatrick, Z. Wang, J. H Sampson et al. "Defining the optimal planning target volume in image-guided stereotactic radiosurgery of brain metastases: Results of a randomized trial". *International Journal of Radiation Oncology Biology Physics*, January 2015, Vol.91(1), pp.100-108
- [29] T. Guido, O. Mattia, L Gaetano et al. "Stereotactic radiosurgery for brain metastases: analysis of outcome and risk of brain radionecrosis". *Radiation Oncology*, May 2011, Vol.6(1), p.48
- [30] S. N Sanghavi, S. S Miranpuri, R. Chappell et al. "Radiosurgery for patients with brain metastases: a multi-institutional analysis, stratified by the RTOG recursive partitioning analysis method". *Int J Radiat Oncol Biol Phys*, 2001, Vol.51, pp. 426-434.
- [31] Thomas, E.M., Popple, R.A., Wu, X. et al "Comparison of plan quality and delivery time between volumetric arc therapy (rapidarc) and gamma knife radiosurgery for multiple cranial metastases". *Neurosurgery*, 2014, Vol.75(4), pp.409-417
- [32] E. Thomas, S. Ollila, R. Popple et al. "An Automated Approach to High-Quality Single-Isocenter Volumetric Modulated Arc Therapy Stereotactic Radiosurgery Treatment Planning on a Linear Accelerator", *International Journal Of Radiation Oncology Biology Physics*, 2016 Oct 1, Vol.96(2)
- [33] L. Lijun, M. Descovich, C. Chuang et al. "Apparatus dependence of normal brain tissue dose in stereotactic radiosurgery for multiple brain metastases". Technical note. *Journal of Neurosurgery*, June 2011, Vol.114(6), pp.1580-1584
- [34] B.J Blonigen, R. D Steinmetz, "Irradiated Volume as a Predictor of Brain Radionecrosis After Linear Accelerator Stereotactic Radiosurgery". *International Journal of Radiation Oncology, Biology and Physics*, 2010, Vol.77(4)
- [35] T. Korytko, T. Radivoyevitch, V. Colussi, et al. "12 GY Gamma Knife radiosurgical volume is a predictor for radiation necrosis in non-AVM intracranial tumors". *Int J Radiat Oncol Biol Phys*, 2006, Vol.64, pp. 419-424
- [36] J.L. Nakamura, L.J. Verhey, V. Smith, et al. "Dose conformality of Gamma Knife radiosurgery and risk factors for complications" *Int J Radiat Oncol Biol Phys*, Vol.51, 2001, pp. 1313-1319
- [37] S. Levergrün, H. Hof, M. Essig, et al. "Radiation-induced changes of brain tissue after radiosurgery in patients with arteriovenous malformations: Correlation with dose distribution parameters" *Int J Radiat Oncol Biol Phys*, 2004, Vol.59, pp. 796-808
- [38] L.A. Nedzi, H. Kooy, E. Alexander III, et al. "Variables associated with the development of complications from radiosurgery of intracranial tumors". *Int J Radiat Oncol Biol Phys*, 1991, Vol.21, pp. 591-599
- [39] D.W. Andrews, C.B. Scott, P.W. Sperduto, et al. "Whole brain radiation therapy with or without stereotactic radiosurgery boost for patients with one to three brain metastases: Phase III results of the RTOG 9508 randomized trial". *Lancet*, 2004, Vol.363, pp. 1665-1672
- [40] J. Voges, H. Treuer, V. Sturm, et al. "Risk analysis of linear accelerator radiosurgery" *Int J Radiat Oncol Biol Phys*, 1996, Vol.36, pp. 1055-1063

- [41] E. Shaw, C. Scott, L. Souhami, et al. "Single dose radiosurgical treatment of recurrent previously irradiated primary brain tumors and brain metastases: Final report of RTOG protocol 90-05". *Int J Radiat Oncol Biol Phys*, 2000, Vol.47 pp. 291-298
- [42] J.C. Flickinger, L.D. Lunsford, D. Kondziolka, et al. "Radiosurgery and brain tolerance: An analysis of neurodiagnostic imaging changes after Gamma Knife radiosurgery for arteriovenous malformations" *Int J Radiat Oncol Biol Phys*, 1992, Vol.23, pp. 19-26
- [43] J.C. Flickinger, D. Kondziolka, L.D. Lunsford, et al. "Development of a model to predict permanent symptomatic postradiosurgery injury for arteriovenous malformation patients". *Int J Radiat Oncol Biol Phys*, 2000, Vol.46, pp. 1143-1148
- [44] J.C. Flickinger, D. Kondziolka, L.D. Lunsford, et al. "A multi-institutional analysis of complication outcomes after arteriovenous malformation radiosurgery" *Int J Radiat Oncol Biol Phys*, 1999, Vol.44, pp. 67-74
- [45] C.A. Valéry, P. Cornu, G. Noël, et al. "Predictive factors of radiation necrosis after radiosurgery for cerebral metastases". *Stereotact Funct Neurosurg*, 2003, Vol. 81, pp. 115-119
- [46] E. Seravalli, P. van Haaren, PP. van Der Toorn et al. "A comprehensive evaluation of treatment accuracy, including end-to-end tests and clinical data, applied to intracranial stereotactic radiotherapy". *Radiotherapy And Oncology*, 2015 Jul, Vol.116(1), pp.131-138
- [47] S-M Chae, G. W Lee et S. H Son "The effect of multileaf collimator leaf width on the radiosurgery planning for spine lesion treatment in terms of the modulated techniques and target complexity". *Radiation Oncology* (London, England), 2014, Vol.9, p.72-72
- [48] Q. Wu, U. Jackie, Z. Wang et al."Impact of collimator leaf width and treatment technique on stereotactic radiosurgery and radiotherapy plans for intra- and extracranial lesions". *Radiation Oncology* (London, England), 2009, Vol.4, p.3-3
- [49] Q. Wu, K. Snyder, C. Liu et al. "Optimization of Treatment Geometry to Reduce Normal Brain Dose in Radiosurgery of Multiple Brain Metastases with Single-Isocenter Volumetric Modulated Arc Therapy". *Scientific Reports*, 2016, Vol.6
- [50] K. Otto, "Volumetric modulated arc therapy: IMRT in a single gantry arc". *Med. Phys.* 2008, Vol.35, pp. 310–317
- [51] C. Huang, L. Ren, J. Kirkpatrick et al. "Treatment of Multiple Brain Metastases Using Stereotactic Radiosurgery with Single-Isocenter Volumetric Modulated Arc Therapy: Comparison with Conventional Dynamic Conformal Arc and Static Beam Stereotactic Radiosurgery". *Medical Physics*, 2012 Jun, Vol.39(6), pp.3854-3854
- [52] K. Stelzer, "Epidemiology and prognosis of brain metastases". *Surgical Neurology International*, 2013, Vol.4(5), p.192-202
- [53] L. Nayak, E. Lee, P. Wen,"Epidemiology of Brain Metastases". *Current Oncology Reports*, 2012 Feb, Vol.14(1), pp.48-54
- [54] A. Wu, G. Lindner, A.H. Maitz et al, "Physics of gamma knife approach on convergent beams in stereotactic radiosurgery". *Int. J. Radiat. Oncol. Biol. Phys.*, 1990, vol.18, pp. 941–949.